NOT FOR PUBLICATION

NEANDC(J)-51/U

INDC(JAP)-37/U

PROGRESS REPORT

(July 1976 to June 1977 inclusive)

September 1977

Editors

T. Fuketa, T. Tamura and S. Kikuchi

Japanese Nuclear Data Committee

Japan Atomic Energy Research Institute

Tokai Research Establishment

Tokai-mura, Ibaraki-ken, Japan

NOT FOR PUBLICATION

NEANDC(J)-51/U

INDC(JAP)-37/U

PROGRESS REPORT

(July 1976 to June 1977 inclusive)

September 1977

Editors

T. Fuketa, T. Tamura and S. Kikuchi

Japanese Nuclear Data Committee

Japan Atomic Energy Research Institute

Tokai Research Establishment

Tokai-mura, Ibaraki-ken, Japan

Editors' Note

This is a collection of reports which have been submitted to the Japanese Nuclear Data Committee at the Committee's request. The request was addressed to the following individuals who might represent or be in touch with groups doing researches related to the nuclear data of interest to the development of the nuclear energy program.

Although the editors tried not to miss any appropriate addressees, there may have been some oversight. Meanwhile, contribution of a report rested with discretion of its author. The coverage of this document, therefore, may not be uniform over the related field of research.

In this progress report, each individual report is generally reproduced as it was received by the JNDC Secretariat, and the editors also let pass some simple obvious errors in the manuscripts if any.

This edition covers a period of July 1, 1976 to June 30, 1977. The information herein contained is of a nature of "Private Communication". Data contained in this report should not be quoted without the author's permission.

Addressees of the request to submit report :

(in Alphabetical order)

1) Electrotechnical Laboratory
Tanashi Branch / 5-4-1, Mukaidai, Tanashi, Tokyo 188
(E. Teranishi)

2) Hiroshima University
Faculty of Science / 1-1-89 Higashi-senda, Hiroshima 730
(Y. Yoshizawa)

3) Hitachi Ltd.
Atomic Energy Research Laboratory / Oozenji, Tama-ku, Kawasaki-shi, Kanagawa 215
(M. Yamamoto)

4) Hokkaido University
Faculty of Engineering / Kitajunijo, Kita-ku, Sapporo 060
(Y. Ozawa, H. Tanaka)

5) Hosei University
2-17-1 Fujimi, Chiyoda-ku, Tokyo 102
(R. Nakasima)

6) Japan Atomic Energy Research Institute
Tokai Research Establishment / Tokai-mura, Naka-gun, Ibaraki 319-11
(T. Abe, H. Amamo, T. Aochi, A. Asami, T. Asaoka, T. Fuketa, Y. Goto, Y. Hamaguchi, M. Hara, K. Harada, M. Hirata, J. Hirota, S. Honma, N. Itoh, S. Katsuragi, H. Kuroi, S. Miyasaka, H. Nakamoto, H. Nakamura, H. Natsume, K. Nishimura, S. Nomura, M. Nozawa, Y. Obata, H. Okashita, S. Tanaka, K. Tsukada, K. Ueno, et al.)

7) Konan University
Faculty of Science / Okamoto, Motoyama-cho, Higashinada-ku, Kobe 658
(K. Yuasa)

8) Kyoto University
   a) Faculty of Engineering / Yoshida Hon-cho, Sakyo-du, Kyoto 606
   (H. Nishihara)

   b) Faculty of Science / Kitashirakawa Oiwaki-cho, Sakyo-ku, Kyoto 606
   (J. Muto)

   c) Institute of Atomic Energy / Gokanosho, Uji-shi, Kyoto 611
   (T. Nishi)

   d) Keage Laboratory of Nuclear Science, Institute for Chemical Research / 2 Torii-cho, Awataguchi, Sakyo-ku, Kyoto 606
   (H. Takekoshi)

   e) Research Reactor Institute / Kumatori, Sennan-gun, Osaka 590-04
   (I. Kimura, K. Okano, S. Okamoto)

9) Kyushu University
   a) Faculty of Engineering / Hakozaki-cho, Higashi-ku, Fukuoka 812
   (Y. Kanda, A. Katase, M. Ohta)

b) Faculty of Science / Hakozaki-cho, Higashi-ku, Fukuoka 812
(A. Isoya, M. Kawai)

10) Mitsubishi Atomic Power Industries, Inc.
Engineering and Development Division / Kitafukuro, Omiya-shi, Saitama 330
(Y. Seki)

11) Nagoya University
Faculty of Engineering / Furo-cho, Chigusa-ku, Nagoya 464
(T. Katoh)

12) National Institute of Radiological Sciences
4-9-1 Anagawa, Chiba 280
(K. Kitao)

13) National Laboratory for High Energy Physics
Ooho-cho, Tsukuba-gun, Ibaraki 300-32
(K. Kato, K. Tskahashi)

14) Nippon Atomic Industry Group Co., Ltd.
NAIG Nuclear Research Laboratory / 4-1. Ukishima-cho, Kawasaki-shi
Kanagawa 210
(S. Iijima)

15) Osaka University
a) Faculty of Engineering / Yamadaue, Suita-shi, Osaka 565
(T. Sekiya, K. Sumita)

b) Faculty of Science / 1-1, Machikaneyama, Toyonaka-shi, Osaka 560
(M. Muraoka, K. Sugimoto)

c) Research Center for Nuclear Physics / Yamadaue, Suita-shi, Osaka
(H. Ikegami, S. Yamabe)

16) Radiation Center fo Osaka Prefecture
704 Shinke-cho, Sakai, Osaka 593
(K. Fukuda)

17) Rikkyo (St. Paul's) University
a) Department of Physics / 3, Ikebukuro, Toshima-ku, Tokyo 171
(I. Ogawa, S. Shirato)

b) Institute for Atomic Energy / 2-5-1, Nagasaka, Yokosuka-shi,
Kanagawa 240-01
(M. Hattori)

18) Ship Research Institute
38-1, 6-chome, Shinkawa, Mitaka-shi, Tokyo 181
(H. Yamakoshi)

19) Sumitomo Atomic Energy Industries, Ltd.
2-10 Kandakaji-cho, Chiyoda-ku, Tokyo 101
(H. Matsunobu)

20) The Institute of Physical and Chemical Research
2-1, Hirosawa, Wako-shi, Saitama 351
(A. Hashizume, H. Kamitsubo)

21) Tohoku University
   a) Faculty of Engineering / Aza-Aoba, Aramaki, Sendai 980
      (T. Momota, K. Sugiyama)

   b) Faculty of Science / Aza-Aoba, Aramaki, Sendai 980
      (S. Morita)

   c) Laboratory of Nuclear Science / 1 Kanayama, Tomisawa, Sendai 982
      (Y. Torizuka)

22) Tokai University
   Faculty of Engineering / 2-28-4 Tomigaya, Shibuya-ku, Tokyo 151
   (Y. Kuroda)

23) Tokyo Institute of Technology
   a) Faculty of Science / 2-12-1 Ohokayama, Meguro-ku, Tokyo 152
      (K. Hisatake, Y. Oda, H. Ohnuma, H. Taketani)

   b) Research Laboratory for Nuclear Reactors / 2-12-1 Ohokayama, Meguro-ku, Tokyo 152
      (N. Yamamuro)

24) University of Tokyo
   a) College of General Education / 3-8-1 Komaba, Meguro-ku, Tokyo 153
      (T. Terasawa)

   b) Faculty of Engineering / 7-3-1 Hongo, Bunkyo-ku, Tokyo 113
      (S. An, A. Sekiguchi)

   c) Faculty of Science / 7-3-1 Hongo, Bunkyo-ku, Tokyo 113
      (Y. Nogami)

   d) Institute for Nuclear Study / 3-2-1 Midori-cho, Tanashi, Tokyo 188
      (T. Hasegawa, Y. Ishizaki, H. Kamitsubo, M. Sakai)

   e) The Institute for Solid Satte Physics / 7-22-1 Roppongi, Minato-ku, Tokyo 106
      (K. Ohno)

25) University of Tsukuba
   Institute of Physics / Ooaza-Saiki, Sakura-mura, Niihari-gun, Ibaraki-ken 300-31
   (J. Sanada)

26) Waseda University
   School of Science and Engineering / 4-170 Nishi-Ohkubo, Shinjuku-ku, Tokyo 160
   (M. Yamada)

TABLE OF CONTENTS

CONTENTS OF THE JAPANESE PROGRESS REPORT INDC(JAP)37U (=NEANDC(J)51U), September 1977

Element S A	Quantity	Lab	Energy(eV) Min	Max	Type	Documentation REF	VOL	PAGE	DATE	Comments
Li 006	Evaluation	JAE	0.0+0	2.0+7	Eval Prog	NEANDC(J)51U		18	Sep 77	KOMODA+.RESULTS GIVEN IN FIGS.
Be 009	Diff Elastic	TOH	3.2+6	7.0+6	Expt Prog	NEANDC(J)51U		63	Sep 77	SAKASE+.DYNAMITRON.TOF.NDG
Be 009	Diff Inelast	TOH	3.2+6	7.0+6	Expt Prog	NEANDC(J)51U		63	Sep 77	SAKASE+.DYNAMITRON.TOF.NDG
B 010	(n,α)	KTO	3.0+3	8.0+4	Expt Prog	NEANDC(J)51U		70	Sep 77	YAMAMURO+.NORMALIZED TO PREVIOUS SIG
O	Nonelastic γ	TOH	1.5+7		Expt Prog	NENADC(J)51U		64	Sep 77	HINO+.DYNAMITRON.RESULTS IN TABLE
F 019	Evaluation	JAE	1.0+5	2.0+7	Eval Prog	NEANDC(J)51U		35	Sep 77	SUGI+.PUBLISHED AS JAERI-M 7253 (77)
Na 023	Nonelastic γ	TOH	1.5+7		Expt Prog	NEANDC(J)51U		64	Sep 77	HINO+.DYNAMITRON.RESULTS IN TABLE
Al 027	Nonelastic γ	TIT	7.2+6		Theo Prog	NEANDC(J)51U		72	Sep 77	SANO+.SPIN-DEPENDENT EVAPORATION MDL
Al 027	Nonelastic γ	TOH	5.8+6	7.2+6	Expt Prog	NEANDC(J)51U		64	Sep 77	HINO+.DYNAMITRON.RESULTS IN TABLE
Al 027	Nonelastic γ	TOH	1.5+7		Expt Prog	NEANDC(J)51U		64	Sep 77	HINO+.DYNAMITRON.RESULTS IN TABLE
Si	Total	KTO	2.0+4	1.6+5	Expt Prog	NEANDC(J)51U		40	Sep 77	KOBAYASHI+.SUBMITTED TO ANN.NUCL.EN.
Si 028	Diff Elastic	JAE	2.1+7		Expt Prog	NEANDC(J)51U		13	Sep 77	YAMANOUTI+.VDG,TOF.CFD OPTMDL CAL
Si 028	Diff Inelast	JAE	2.1+7		Expt Prog	NEANDC(J)51U		13	Sep 77	YAMANOUTI+.VDG,TOF.CFD OPTMDL CAL
S 032	Diff Elastic	JAE	2.2+7		Expt Prog	NEANDC(J)51U		13	Sep 77	YAMANOUTI.PUBLISHED IN NP/A283(77)23
S 032	Diff Inelast	JAE	2.2+7		Expt Prog	NEANDC(J)51U		13	Sep 77	YAMANOUTI.PUBLISHED IN NP/A283(77)23
Cl	Nonelastic γ	TOH	1.5+7		Expt Prog	NEANDC(J)51U		64	Sep 77	HINO+.DYNAMITRON.RESULTS IN TABLE
Ca 040	Nonelastic γ	TIT	7.2+6		Theo Prog	NEANDC(J)51U		72	Sep 77	SANO+.SPIN-DEPENDENT EVAPORATION MDL.
Ti 048	(n,p)	TIT	Thrsh	2.0+7	Theo Prog	NEANDC(J)51U		74	Sep 77	ISOGAI+.EVAP+PRECOMP MDL.FIG
V 051	(n,p)	TIT	Thrsh	2.0+7	Theo Prog	NEANDC(J)51U		74	Sep 77	ISOGAI+.EVAP+PRECOMP MDL.FIG
Cr 052	(n,p)	TIT	Thrsh	2.0+7	Theo Prog	NEANDC(J)51U		74	Sep 77	ISOGAI+.EVAP+PRECOMP MDL.FIG
Fe	Total	KTO	2.2+4	2.5+4	Expt Prog	NEANDC(J)51U		40	Sep 77	KOBAYASHI+.SUBMITTED TO ANN. NUCL.EN.
Fe	Nonelastic γ	TOH	1.5+7		Expt Prog	NEANDC(J)51U		64	Sep 77	HINO+.DYNAMITRON.RESULTS IN TABLE
Fe	(n,γ)	JAE	+1	+3	Expt Prog	NEANDC(J)51U		9	Sep 77	OHKUBO.PUBLISHED IN NIM 143(77) 173
Fe 056	Nonelastic γ	TIT	7.2+6		Theo Prog	NEANDC(J)51U		72	Sep 77	SANO+.SPIN-DEPENDENT EVAPORATION MDL
Fe 056	(n,p)	TIT	Thrsh	2.0+7	Theo Prog	NEANDC(J)51U		74	Sep 77	ISOGAI+.EVAP+PRECOMP MDL.FIG
Ni 058	(n,p)	TIT	Thrsh	2.0+7	Theo Prog	NEANDC(J)51U		74	Sep 77	ISOGAI+.EVAP+PRECOMP MDL.FIG
Cu	Nonelastic γ	TOH	1.5+7		Expt Prog	NEANDC(J)51U		64	Sep 77	HINO+.DYNAMITRON.RESULTS IN TABLE
Cu	Diff Inelast	KYU	1.4+7		Expt Prog	NEANDC(J)51U		56	Sep 77	IRIE+.SIG CFD PRECOMPOUND MODEL
Cu	(n,γ)	JAE	+1	+3	Expt Prog	NEANDC(J)51U		9	Sep 77	OHKUBO.PUBLISHED IN NIM 143(77) 173
As	Diff Inelast	KYU	1.4+7		Expt Prog	NEANDC(J)51U		56	Sep 77	IRIE+.SIG CFD PRECOMPOUND MODEL
Zr 090	Diff Elastic	JAE	5.9+6	7.8+6	Expt Prog	NEANDC(J)51U		11	Sep 77	TANAKA+.VDG,TOF.30DEG TO 150DEG.
Zr 090	Diff Inelast	JAE	5.9+6	7.8+6	Expt Prog	NEANDC(J)51U		11	Sep 77	TANAKA+.VDG.TOF.30DEG TO 150DEG.
Zr 090	(n,2n)	KYU	1.5+7		Expt Prog	NEANDC(J)51U		60	Sep 77	FUJINO+.ACT SIG=805+-58MB FOR G.S.
Zr 090	(n,2n)	KYU	1.5+7		Expt Prog	NEANDC(J)51U		60	Sep 77	FUJINO+.ACT SIG=86+-8MB FOR META
Zr 090	(n,p)	KYU	1.5+7		Expt Prog	NEANDC(J)51U		60	Sep 77	FUJINO+.ACT SIG=9.0+-0.8MB FOR META
Zr 090	(n,α)	KYU	1.5+7		Expt Prog	NEANDC(J)51U		60	Sep 77	FUJINO+.ACT SIG=4.1+-0.3MB FOR META
Zr 091	(n,p)	KYU	1.5+7		Expt Prog	NEANDC(J)51U		60	Sep 77	FUJINO+.ACT SIG=21.4+-2.2MB FOR META
Zr 092	Diff Elastic	JAE	5.9+6	7.8+6	Expt Prog	NEANDC(J)51U		11	Sep 77	TANAKA+.VDG.30-150DEG.TOF-SPECTR-FIG
Zr 092	Diff Inelast	JAE	5.9+6	7.8+6	Expt Prog	NEANDC(J)51U		11	Sep 77	TANAKA+.VDG.30-150DEG.TOF-SPECTR-FIG
Zr 092	(n,p)	KYU	1.5+7		Expt Prog	NEANDC(J)51U		60	Sep 77	FUJINO+.ACT SIG=20.1+-1.5MB

Element S A	Quantity	Lab	Energy(eV) Min	Max	Type	Documentation Ref Vol	Page	Data	Comments
Zr 094	(n,p)	KYU	1.5+7		Expt Prog	NEANDC(J)51U	60	Sep 77	FUJINO+.ACT SIG=10.7+-1.1MB
Zr 094	(n,α)	KYU	1.5+7		Expt Prog	NEANDC(J)51U	60	Sep 77	FUJINO+.ACT SIG=6.3+-0.5MB
Zr 096	(n,α)	KYU	1.5+7		Expt Prog	NEANDC(J)51U	60	Sep 77	FUJINO+.ACT SIG=2.4+-0.3MB
Nb	Diff Inelast	KTU	1.4+7		Expt Prog	NEANDC(J)51U	56	Sep 77	IRIE+.SIG CFD PRECOMPOUND MODEL
Nb 093	Nonelastic γ	TIT	7.2+6		Theo Prog	NEANDC(J)51U	72	Sep 77	SANO+.SPIN-DEPENDENT EVAPORATION MDL
Nb 093	(n,γ)	KTO	3.0+3	8.0+4	Expt Prog	NEANDC(J)51U	70	Sep 77	YAMAMURO+.AGREED WITH MACKLIN DATA
Nb 093	(n,p)	TIT	Thrsh	2.0+7	Theo Prog	NEANDC(J)51U	74	Sep 77	ISOGAI+.EVAP+PRECOMP MDL.FIG
Mo	(n,γ)	JAE	+1	+3	Expt Prog	NEANDC(J)51U	9	Sep 77	OHKUBO.PUBLISHED IN NIM 143(77) 173
Mo 092	(n,2n)	KYU	1.5+7		Expt Prog	NEANDC(J)51U	60	Sep 77	FUJINO+.ACT SIG=11.8+-1.2MB FOR META
Mo 092	(n,p)	KYU	1.5+7		Expt Prog	NEANDC(J)51U	60	Sep 77	FUJINO+.ACT SIG=68+-6MB FOR META
Mo 092	(n,α)	KYU	1.5+7		Expt Prog	NEANDC(J)51U	60	Sep 77	FUJINO+.ACT SIG=20.0+-1.6MB FOR G.S.
Mo 092	(n,α)	KYU	1.5+7		Expt Prog	NEANDC(J)51U	60	Sep 77	FUJINO+.ACT SIG=5.6+-0.5MB FOR META
Mo 094	(n,2n)	KYU	1.5+7		Expt Prog	NEANDC(J)51U	60	Sep 77	FUJINO+.ACT SIG=2.4+-0.2MB FOR META
Mo 096	(n,p)	KYU	1.5+7		Expt Prog	NEANDC(J)51U	60	Sep 77	FUJINO+.ACT SIG=18.1+-1.4MB
Mo 097	(n,p)	KYU	1.5+7		Expt Prog	NEANDC(J)51U	60	Sep 77	FUJINO+.ACT SIG=19.2+-1.4MB FOR G.S.
Mo 098	(n,p)	KYU	1.5+7		Expt Prog	NEANDC(J)51U	60	Sep 77	FUJINO+.ACT SIG=3.6+-0.3MB
Mo 098	(n,p)	TIT	Thrsh	2.0+7	Theo Prog	NEANDC(J)51U	74	Sep 77	ISOGAI+.EVAP+PRECOMP MDL.FIG
Mo 100	(n,2n)	KYU	1.5+7		Expt Prog	NEANDC(J)51U	60	Sep 77	FUJINO+.ACT SIG=1420+-100MB
Ag	Diff Inelast	KYU	1.4+7		Expt Prog	NEANDC(J)51U	56	Sep 77	IRIE+.SIG CFD PRECOMPOUND MODEL
Sb	(n,γ)	JAE	+1	+3	Expt Prog	NEANDC(J)51U	9	Sep 77	OHKUBO.PUBLISHED IN NIM 143(77) 173
I 127	(n,γ)	KTO	3.0+3	8.0+4	Expt Prog	NEANDC(J)51U	70	Sep 77	YAMAMURO+.NDG
Cs 133	(n,γ)	KTO	5.5+4		Expt Prog	NEANDC(J)51U	43	Sep 77	FUJITA+.SI-FILTER.S=0.37+-0.033B
Cs 133	(n,γ)	KTO	1.5+5		Expt Prog	NENADC(J)51U	43	Sep 77	FUJITA+.SI-FILTER.S=0.21+0.017B
Cs 133	(n,γ)	KTO	3.0+3	8.0+4	Expt Prog	NEANDC(J)51U	70	Sep 77	YAMAMURO+.SIG GIVEN IN FIG
Tb 159	Reson Params	JAE	+1	1.2+3	Expt Prog	NEANDC(J)51U	7	Sep 77	OHKUBO+.SO=1.5E-4,WG=0.105EV,D=4.3EV
Ho 165	(n,γ)	KTO	3.0+3	8.0+4	Expt Prog	NEANDC(J)51U	70	Sep 77	YAMAMURO+.AGREED WITH MACKLIN DATA
Ta 181	Nonelastic γ	TIT	7.2+6		Theo Prog	NEANDC(J)51U	72	Sep 77	SANO+.SPIN-DEPENDENT EVAPORATION MDL
Ta 181	(n,γ)	KTO	3.0+3	8.0+4	Expt Prog	NEANDC(J)51U	70	Sep 77	YAMAMURO+.NDG
Ta 181	(n,p)	TIT	Thrsh	2.0+7	Theo Prog	NEANDC(J)51U	74	Sep 77	ISOGAI+.EVAP+PRECOMP MDL.FIG
Pb	Nonelastic γ	TIT	7.2+6		Theo Prog	NEANDC(J)51U	72	Sep 77	SANO+.SPIN-DEPENDENT EVAPORATION MDL
Pb	Nonelastic γ	TOH	1.5+7		Expt Prog	NEANDC(J)51U	64	Sep 77	HINO+.DYNAMITRON.RESULTS IN TABLE
Th 232	Fission	KTO	Fiss		Expt Prog	NEANDC(J)51U	46	Sep 77	KOBAYASHI.SUBMITTED TO ANN.NUCL.EN.
Pa 231	Fission	KTO	Fiss		Expt Prog	NEANDC(J)51U	48	Sep 77	KOBAYASHI+.FISS-SPECTR AVERAGED SIG
U 233	Fiss Yield	KTO	Maxwl		Expt Prog	NEANDC(J)51U	38	Sep 77	NISHI+.INDEP-Y OF I-131,132,133.134
U 235	Fission	JAE	Maxwl		Theo Prog	NEANDC(J)51U	33	Sep 77	UMEZAWA+.INDEP YIELD OF CS-134
U 235	Fiss Yield	KTO	Maxwl		Expt Prog	NEANDC(J)51U	38	Sep 77	NISHI+.INDEP-Y OF I-131,132,133,134
U 235	Fiss Prod γ	KTO	Maxwl		Expt Prog	NEANDC(J)51U	54	Sep 77	KISO+.PUBLISHED IN NST 14(77)482
U 238	Total	JAE	+1	+4	Expt Prog	NEANDC(J)51U	5	Sep 77	ASAMI+.SUBMITIED TO NUCL.INSTR.METH.
U 238	Reson Params	JAE	2.0+1	3.0+4	Expt Prog	NEANDC(J)51U	6	Sep 77	NAKAJIMA.SUBMITTED TO ANN.NUCL.ENERG
U 238	(n,γ)	KTO	5.5+4		Expt Prog	NEANDC(J)51U	43	Sep 77	FUJITA+.SI-FILTER.S=0.34+-0.05B

Element S A	Quantity	Lab	Energy (eV) Min	Max	Type	Documentation Ref Vol	Page	Date	Comments
U 238	(n,γ)	KTO	1.5+5		Expt Prog	NEANDC(J)51U	43	Sep 77	FUJITA+.SI-FILTER.S=0.187+-0.017B
U 238	(n,α)	KTO	3.0+3	8.0+4	Expt Prog	NEANDC(J)51U	70	Sep 77	YAMAMURO+.NDG
Pu 239	Fiss Yield	KTO	Maxwl		Expt Prog	NEANDC(J)51U	38	Sep 77	NISHI+.INDEP-Y OF I-132,133,134
Am 243	Evaluation	JAE	1.0-5	1.6+7	Eval Prog	NEANDC(J)51U	22	Sep 77	IGARASI+.EVALUATED CURVES IN FIG.
Cm 244	Evaluation	JAE	1.0-5	1.6+7	Eval Prog	NEANDC(J)51U	22	Sep 77	IGARASI+.EVALUATED CURVES IN FIG.
Many	Reson Params	JAE	+1	+3	Expt Prog	NEANDC(J)51U	8	Sep 77	OHKUBO.SUBMITTED TO NUCL.SCI.ENG.
Many	Reson Params	JAE			Theo Prog	NEANDC(J)51U	14	Sep 77	IDENO.PERIODIC STRUCTURE IN RES-LVLS
Many	Reson Params	JAE			Theo Prog	NEANDC(J)51U	16	Sep 77	IDENO.EMPHASYZES THE PERIODICITY
Many	(n,2n)	KYU	1.5+7		Theo Prog	NEANDC(J)51U	59	Sep 77	KUMABE.PUBLISHED IN NST 14(77)460
Many	(n,p)	KYU	1.4+7		Theo Prog	NEANDC(J)51U	57	Sep 77	KUMABE+.SIGS CFD PRECOMPOUND MODEL
Many	(n,α)	KYU	1.4+7		Theo Prog	NEANDC(J)51U	57	Sep 77	KUMABE+.SIGS CFD PRECOMPOUND MODEL

I. Hiroshima University

Department of Physics, Faculty of Science

I-1 Precision Measurements of Gamma-Ray Intensities

Y. Yoshizawa, Y. Iwata, T. Katoh*, J. Ruan**, T. Kojima**
and Y. Kawada***

Gamma-ray intensities were determined with Ge(Li) detectors in the energy region 280-1840 keV. The detectors were calibrated by using standard sources of ^{22}Na, ^{46}Sc, ^{54}Mn, ^{60}Co, ^{85}Sr, ^{88}Y, ^{134}Cs and ^{203}Hg. Decay rates of these sources were measured with errors of 0.1~0.5 % by means of the β-γ X-γ coincidence method. In addition, the cascade gamma-ray sources of ^{108m}Ag was used. Measurements were performed at Hiroshima and Nagoya. We took care of the gamma-ray absorption, the source position and the dead time in measurements and of the peak integration and the background subtraction in analysis. Several equations of the efficiency curve were examined. The best efficiency curve was obtained with the accuracy of 0.5 %.

Relative intensities and intensities per decays were determined with errors of about 0.5 % for ^{88}Y, ^{134}Cs, ^{152}Eu and ^{207}Bi. Results are shown in Tables 1, 2 and 3.

---

* Faculty of Engineering, Nagoya University, Nagoya

** Faculty of Science, Rikkyo University, Tokyo

*** Electrotechnical Laboratory, Tanashi, Tokyo

Table 1. Gamma-ray intensities of ^{88}Y and ^{207}Bi

Nuclide	Energy (keV)	Relative intensity (%)	Intensity per decay (%)
^{88}Y	1836	100	99.24(7)
	898	94.2(3)	93.5(3)
^{207}Bi	1064	75.5(3)	73.8(3)
	897	0.121(12)	0.118(12)
	570	100	97.74(3)

Table 2. Gamma-ray intensities of ^{134}Cs

Energy (keV)	Relative intensity (%)	Intensity per decay (%)
1365	3.082(20)	3.009(19)
1168	1.827(9)	1.784(9)
1038	1.005(7)	0.981(6)
802	8.90(4)	8.69(4)
796	87.4(4)	85.48(5)
605	100	97.63(6)
569	15.81(7)	15.43(7)
563	8.59(4)	8.38(4)

Table 3. Relative gamma-ray intensities of ^{152}Eu

Energy (keV)	Relative intensity (%)	Energy (keV)	Relative intensity (%)	Energy (keV)	Relative intensity (%)
296	3.24(3)	679	3.528(29)	964	108.3(6)
329	1.089(22)	689	6.50(5)	1005	5.33(5)
344	196.0(12)	719	2.59(3)	1086	74.6(3)
368	6.38(5)	765	1.478(27)	1090	12.92(8)
411	16.81(10)	779	96.3(4)	1109	1.54(7)
444	23.36(14)	810	2.43(3)	1112	100
488	3.165(27)	842	1.30(3)	1213	10.61(7)
504	1.202(20)	867	31.51(14)	1250	1.36(3)
564	3.78(6)	901	0.624(25)	1299	12.09(7)
586	3.39(5)	919	3.22(3)	1408	155.2(9)
657	1.091(22)	926	2.136(29)	1528	2.090(23)
675	1.450(24)	931	0.572(24)		

I-2 Evaluation of Gamma-Ray Intensities

Y. Yoshizawa, H. Inoue, M. Hoshi, K. Shizuma and Y. Iwata

Relative gamma-ray intensities and intensities per decays were evaluated for eight nuclides. Intensities per decays are nearly 100 % for strong gamma rays of ^{24}Na, ^{57}Co, ^{85}Sr, ^{88}Y, ^{108m}Ag, ^{139}Ce and ^{207}Bi. These gamma rays are useful for gamma-ray intensity calibration. Gamma-ray intensities of ^{144}Ce and ^{144}Pr were in requests of the atomic fuel problem. Evaluated values are listed in Tables 1 and 2.

Table 1. Gamma-ray intensities of primary standards

Nuclide	Energy (keV)	Relative intensity (%)	Intensity per decay (%)
^{24}Na	1368.6	100.0000	99.9922±0.0010
	2754	99.8836±0.0035	99.8758±0.0034
^{57}Co	122.06		85.4 ±0.6
^{85}Sr	514.0		99.0 ±0.3
^{88}Y	1836		99.24 ±0.07
^{108m}Ag	434.0	99.36 ±0.09	90.6 ±0.6
	614.4	99.88 ±0.04	91.1 ±0.6
	723.0	100.00	91.2 ±0.6
^{139}Ce	165.85		79.83 ±0.20
^{207}Bi	569.7		97.71 ±0.03

Table 2. Other gamma-ray intensities

Nuclide	Energy (keV)	Relative intensity (%)	Intensity per decay (%)
^{57}Co	14.41	10.64±0.22	9.09±0.18
	122.06	100.0	85.4 ±0.6
	136.47	12.6 ±0.6	10.8 ±0.5
^{88}Y	898.0	95.0 ±0.5	94.3 ±0.5
	1836	100.0	99.24±0.07
^{144}Ce	80.12	15.0 ±1.0	1.5 ±0.1
	133.53	100	10.1 ±0.7
^{144}Pr	696.5	100	1.51±0.06
	1489	20.0 ±0.6	0.30±0.05
	2186	50.2 ±1.3	0.76±0.04
^{207}Bi	569.7	100.0	97.71±0.03
	1064	76.8 ±2.0	75.0 ±2.0

II. JAPAN ATOMIC ENERGY RESEARCH INSTITUTE

A. Linac Laboratory, Division of Physics

II-A-1

New Method for Precise Background Determination in Neutron Transmission Measurements with a Linac

A. Asami and Y. Nakajima

A paper on this subject was submitted for publication in "Nuclear Instruments and Methods" with an abstract as follows:

The black resonance technique is widely used for background determination in neutron corss section measurements in the low energy region. However it was found that the background thus determined depends on the black resonance samples.

To overcome this difficulty a new method has been developed. It is to deduce the background by analysing neutron spectra with and without the black resonance samples. Examples are given of ^{238}U transmission measurements.

II-A-2 ## Neutron Resonance Parameters of ^{238}U

Y. Nakajima

A paper on this subject was submitted to Annals of Nuclear Energy with an abstract as follows:

Neutron transmission measurements on natural uranium samples were performed in the energy region from 20 eV up to 30 keV on a 190 m flight path of the JAERI 120 MeV linac neutron time-of-flight spectrometer. Samples were all metallic slabs with three thicknesses of 0.00725, 0.0144 and 0.0236 atoms/barn, respectively. One of them was cooled down to 77 °K to reduce Doppler broadening effect. The best nominal resolution of the measurements was 0.3 nsec/m. Special attention has been paid to background determination because its shape was found to depend on the thickness of the sample in the beam. Resonance parameters Γ_n^o are obtained for 180 resonances in the energy region up to 4.7 keV with the Atta-Harvey area-analysis programme. Excluding p-wave resonances assigned by F. Corvi et al., the average level spacing, the average reduced neutron width and the strength function were determined to be $\bar{D}$ = 21.9 $\pm$ 1.5 eV, $\overline{\Gamma_n^o}$ = 2.47 $\pm$ 0.33 meV and So = (1.13 $\pm$ 0.13) x 10^{-4}, respectively. The statistics of the level spacings are in agreement with those predicted by the theory of Dyson and Mehta and are inconsistent with an uncorrelated Wigner distribution. Results are compared with currently available experimental data.

II-A-3 Neutron Resonances in Tb-159

M. Ohkubo and Y. Kawarasaki

An experiment on the neutron resonances in Tb-159 was carried out using the JAERI linac time of flight facility. Two simultaneous measurements were performed; transmission and capture measurements on terbium of two different sample thicknesses, using a ^{6}Li glass scintillator and a Moxon-Rae detector, at the 47-m station of the TOF facility. Transmission data were analysed with area analysis up to 1.2 keV, and the capture data with a Monte=Carlo program CAFIT to obtain $2g\Gamma_n^0$, Γ, and $\Gamma\gamma$. Spin determinations were also made for large resonances. Average level spacing $\langle D \rangle$ and s-wave strength function So are obtained; $\langle D \rangle = 4.3 \pm 0.4$ eV below 500 eV, and $S_0 = (1.55 \pm 0.15)10^{-4}$ for 205 levels below 1.2 keV. Average radiation width is also obtained to be $\langle \Gamma\gamma \rangle = 105 \pm 7$ meV for lower 22 levels.

II−A−4

Neutron Capture Probabilities for Thick Samples at Resonance Energies

M. Ohkubo

A paper on this subject was submitted to Nucl. Sci. Eng., with an abstract as follows:

Capture and scattering probabilities for neutrons impinging on thick samples are measured by the JAERI linac TOF spectrometer, and are compared with those by Monte-Carlo calculation. Sweeping the incident neutron energy, the capture probability shows peaks at resonance energies in the case of thin sample, whereas it shows dips for a thick sample, i.e. saturation occurs just at resonance energies. This saturation phenomenon is analysed by Monte-Carlo calculation, for a distribution of path length of incident neutrons in the sample until capture in the sample.
The saturation values of capture probability at resonance energies P_{co} are defined, and its dependence on the resonance parameters Γ_n/Γ is examined. The relations between P_{co} and Γ_n/Γ, with parameters including recoil energy, are obtained by Monte-Carlo calculation. The relations are verified by the measurements of P_{co} for many resonances of various Γ_n/Γ values. With the relation Γ_n/Γ can be determined from P_{co}, which is not sensitive to sample thickness.

II-A-5

Recoil Energy and Effective Mass Determinations from Neutron Capture Line Shapes for Narrow Resonances

M. Ohkubo

A paper on this subject was published in "Nuclear Instruments and Methods" 143(1977) 173 with an abstract as follows:

Recoil energies and effective masses of Fe, Cu, Mo, and Sb are determined from the neutron capture line shapes for narrow resonances in rather thick samples, in which resonance capture without scattering and that after one scattering are predominant. Mass numbers obtained are consistent with the values of free atoms within experimental errors.

II−A−6

Reconstruction of the JAERI-linac first accelerator section

A. Asami, K. Mashiko, M. Kitajima
Y. Nobusaka, N. Akiyama and T. Shohji

Deterioration of the first accelerating waveguide of the linac had taken place in these years, so the reconstruction of this accelerator section was undertaken, which was recently completed.

In the reconstruction, a buncher and its associated equipments, such as an RF source a vacuum system, etc., were newly fabricated, and also the old accelerating waveguide was replaced by a new one. In the old accelerator, a single step buncher and a regular accelerating section constituted the first accelerating waveguide as one body. The new buncher is of a multi-step type, and operates with an RF power of 8 MW. It accelerates electrons up to 3 MeV with the current of 2A.

The performance of the linac obtained as a result of this reconstruction is as follows:
For a pulse duration of one or two microseconds the peak current of the accelerated beam is 610 mA with the energy of 84 Mev. For a pulse duration of 30 nanoseconds the peak current is 1.8 A with the energy of 100 Mev.

B. Nuclear Physics Laboratory, Division of Physics

II-B-1 Fast Neutron Scattering from ^{90}Zr and ^{92}Zr

S. Tanaka and Y. Yamanouti

Differential cross sections for elastic and inelastic scattering from ^{90}Zr and ^{92}Zr have been measured at neutron energies of 5.90, 6.95 and 7.75 MeV. The measurement was made in the angular region 30° - 150° in 5° or 10° steps by useing a multi-angle TOF spectrometer with four detectors. Flight paths were taken as 5.9 m. The absolute cross section scale was fixed with reference to the n-p scattering by observing the neutron group from a thin polyethylene scatterer. Each of the ^{90}Zr and ^{92}Zr samples was a metalic right cylinder 2 cm in diameter and about 2 cm high.

A typical TOF spectrum is shown in Fig. 1. Crosses represent the background spectrum. The lines in the figure indicate positions of peaks expected from the known states in ^{92}Zr. As is expected from the figure, at least inelastic cross sections for the first 2^+ and 3^- states will be obtained in addition to the elastic cross sections.

At present, data analysis is in progress.

The authors are greatly indebted for the use of ^{90}Zr and ^{92}Zr samples in the ORNL pool by the courtesy of NEANDC and ERDA.

Fig. 1 TOF spectrum of neutrons elastically and inelastically scattered from ^{92}Zr.

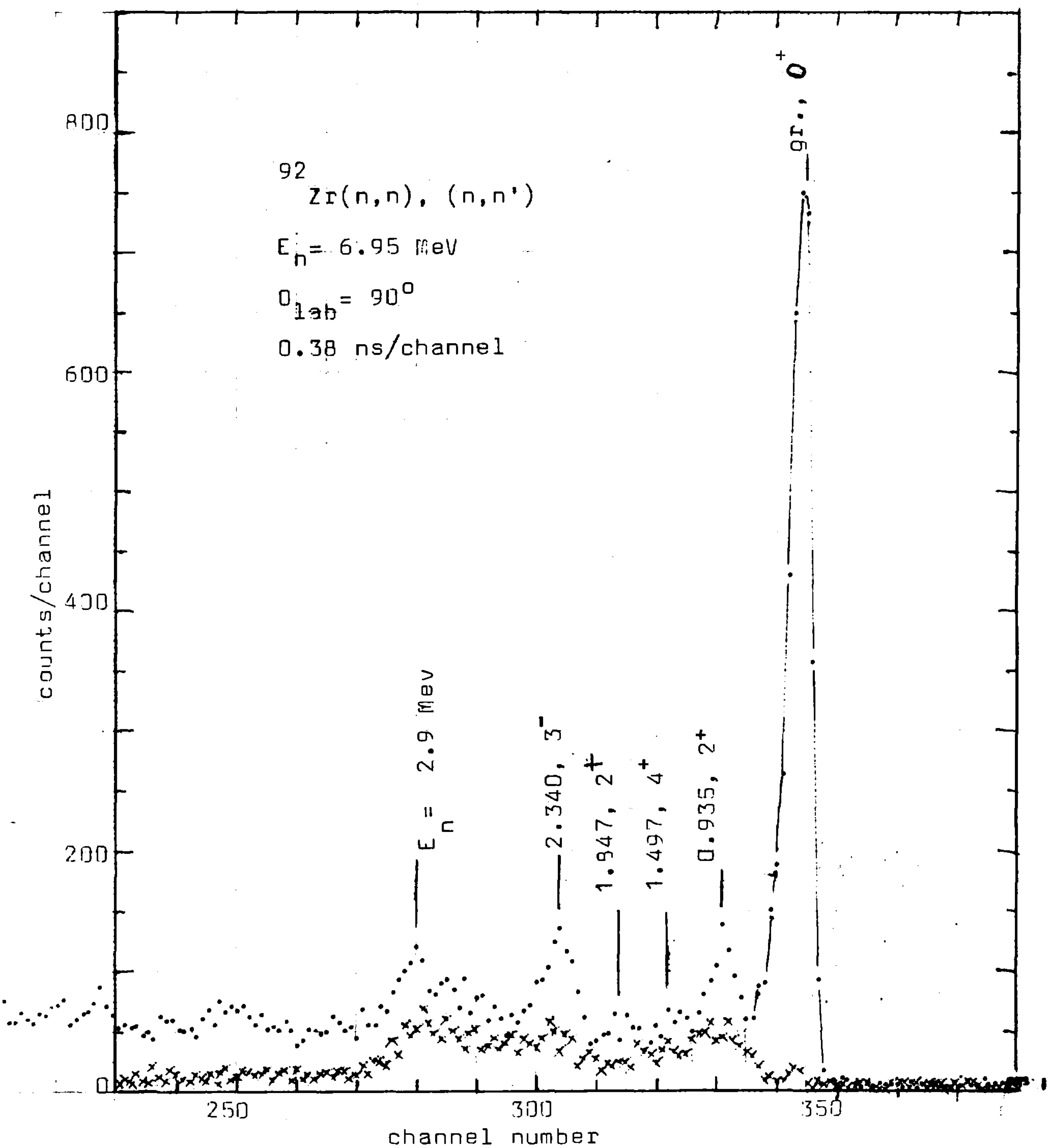

II-B-2 Elastic and inelastic scattering of 21.5 MeV neutrons from ^{32}S

Y. Yamanouti

The paper on this subject is published in Nuclear Physics A 283 (1977) 23.

II-B-3 Elastic and inelastic scattering of 21.0 MeV neutrons from ^{28}Si

Y. Yamanouti and S. Tanaka

Differential cross sections for elastic and inelastic scattering of 21.0 MeV neutrons from ^{28}Si were measured over the angular range from 20° to 145° in order to study the reaction mechanism and collective properties of the low-lying excited states. The 21.0 MeV neutrons were generated by the $^{3}H(d,n)^{4}He$ reaction using a pulsed beam from the JAERI 5.5 MV Van de Graaff accelerator. The time-of-flight technique was employed to detect neutrons.

The experimental cross sections are shown in fig.1 together with results of theoretical calculations. The experimental cross sections were analyzed by the optical model and the coupled-channel (CC) calculations based on the rotational model. The CC calculations were performed by using the code JUPITOR-1. As is seen in fig.1, the experimental cross sections are well reproduced by the coupled-channel calculations based on the rotational model.

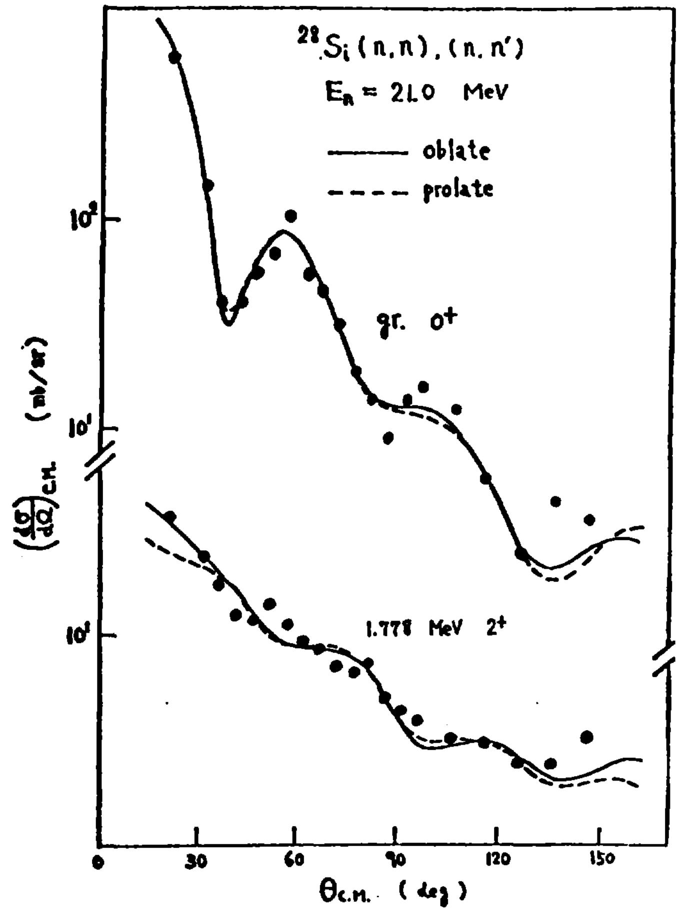

Fig. 1

II-B-4 <u>Does the Periodicity of Level Distributions come from the Dyson-Mehta Theory?</u>

K. Ideno

The paper on this subject was the contribution to the International Conference on Nuclear Structure held at Tokyo, Japan in September 5 - 10, 1977 with an abstract as follows:

Analyzing neutron resonance data, we have found periodic level structure in a wide variety of nuclei, among which rare-earth nuclei occupy a large part [1,2]. On the other hand, several statistics such as the Dyson-Mehta Δ statistics are reported to be consistent with the theory of random matrices [3]. Accordingly it is important to see whether the periodic structure can be predicted from the random matrix hypothesis or not. For this purpose we compare the mean value and variance of $A_m(x)$ between two ensembles: one obeying to the Poisson distribution and the other the orthogonal ensemble [4]. Here $A_m(x)$ is a level statistic which is devised to detect a dominant period in the level distribution [1].

Since $A_m(x)$ is the sum of $A_1(x)$, $A_1(2x)$,..., $A_1(mx)$, we can estimate the mean value and variance for higher order m if we know the results for the order m = 1. The mean value is

$$\langle A_1(x)\rangle = (N\langle D\rangle - x)\int_{(x-\Delta E/2)/\langle D\rangle}^{(x+\Delta E/2)/\langle D\rangle} R_2(y)\,dy\,,$$

where N is the number of levels, $\langle D\rangle$ the mean level distance, ΔE the uncertainity in x. $R_2(x)$ is the two-level correlation function. For $x \gtrsim 1$, $R_2(x) \approx 1$ for both ensembles. Hence the mean values coincide well for not so small x. Using the analytical expressions for two- to four-level correlation functions [5], we have obtained the numerical estimates for the variances with $\Delta E/\langle D\rangle = 0.1$. The results are shown in the figure, where $\sigma = \sqrt{\mathrm{var}\ A_m(x)}$. The variance for the orthogonal ensemble is slightly less than that for the Poisson distribution, but there is almost no difference. This holds also for the variance of $A_m(x)$ with higher m. In the actual resonance data $A_m(x)$ has sharp peaks at regular intervals, their heights being too big than expected from the random levels. Therefore the observation of the periodic level structure does not agree with the predictions of the random matrix hypothesis.

1) K. Ideno et al., J. Phys. Soc. Japan <u>30</u> (1971) 620, <u>37</u> (1974) 581.
2) K. Izumo, Prog. Theor. Phys. <u>54</u> (1975) 1378.
3) H. I. Liou et al., Phys. Rev. <u>C5</u> (1972) 974.

4) F. J. Dyson, J. Math. Phys. 3 (1962) 166.

5) F. J. Dyson, Comm. Math. Phys. 19 (1970) 235.

M. L. Mehta, Private communication.

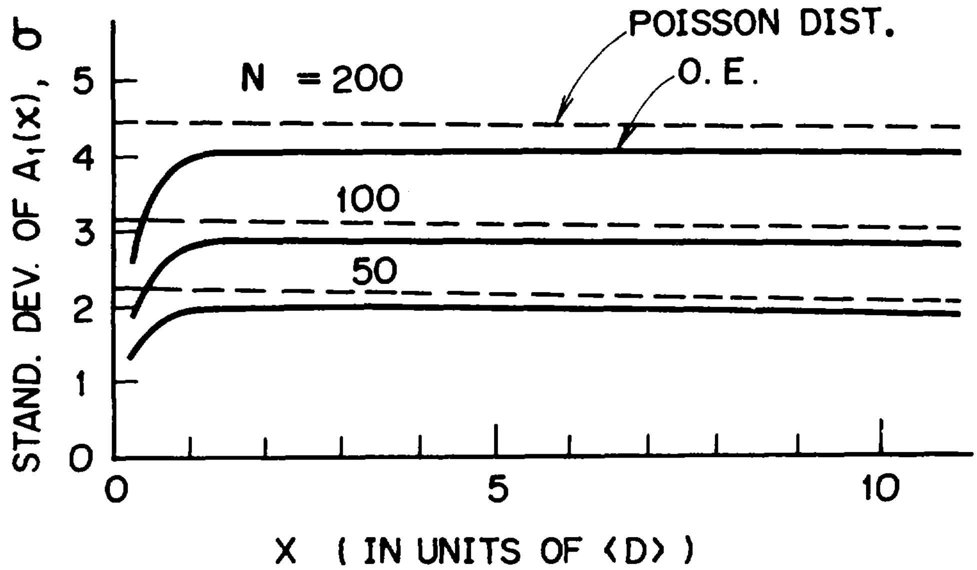

II-B-5 Superfine Structure in Neutron Resonances and its Relation to Zero Neutron Energy

K. Ideno

The paper on this subject was the contribution to the International Conference on Nuclear Structure held at Tokoy, Japan in September 5 - 10, 1977 with an abstract as follows:

Observed level sequences for medium and heavy nuclei can be decomposed into overlapping series of periodic levels with particular dominant periods [1], which play an important role in the compound reaction process [2]. The period x is determined within the uncertainity ΔE, where the ratio between the two quantities is $\Delta E/x = 0.05$ to 0.1 in most of cases. To classify nuclei according to structural resemblance, we have applied a frequency analysis $A_m(x)$ [1] to the combined resonance energies of a pair of nuclei which have a common period: ^{112}Cd + ^{114}Cd (110 eV), ^{113}Cd + ^{141}Pr (55 eV), ^{114}Cd + ^{174}Yb (222 eV), ^{143}Nd + ^{166}Er (66 eV), ^{149}Sm + ^{155}Gd (2.65 eV), ^{152}Sm + ^{154}Sm (154 eV), ^{154}Gd + ^{167}Er (12.8 eV) and ^{170}Er + ^{174}Yb (146 eV). The mixing of the levels has been made in two ways: with or without a relative shift of the level energies between a pair of the nuclei. In the latter case we treat the zero neutron energy as a common starting point for the levels of the two nuclei. Figure shows the height of $A_{10}(x = 55\text{ eV})$ as a function of the relative shift for ^{113}Cd + ^{141}Pr, where $E < 2000$ eV, $\Delta E = 2$ eV and the number of levels is $N = 60$. The period of 55 eV appears dominant at the relative shifts of 0 and 55 eV while less dominant at the other relative shifts. For the other examples of the hybrid nuclei listed above the same thing holds true: The common period is still dominant at the zero relative shift and at the relative shifts equal to the integral multiples of the period (on phase), and it is less dominant at the other relative shifts (off phase). Thus the excitation quanta (periods) for these nuclei are cooperatively built on the zero neutron energy, i.e. on the neutron separation energy.

1) K. Ideno and M. Ohkubo, J. Phys. Soc. Japan 30 (1971) 620, 37 (1974) 581.

2) K. Izumo, Prog. Theor. Phys. 54 (1975) 1378, 55 (1976) 1827.

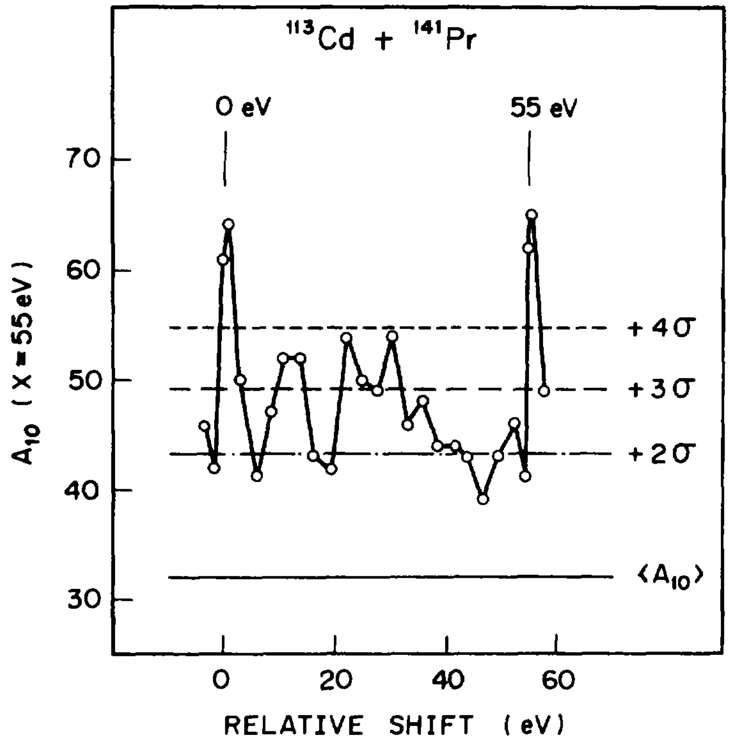

113Cd + 141Pr
0 eV
55 eV
70
60
50
40
30
A10 (X = 55 eV)
+4σ
+3σ
+2σ
⟨A10⟩
0
20
40
60
RELATIVE SHIFT (eV)

C. Nuclear Data Center, Division of Physics and Working Groups of Japanese Nuclear Data Committee

II-C-1 Neutron Cross Sections of ^6Li

S. Komoda* and S. Igarasi

We had tried[1] to determine energies, spins, parities and widths for the excited levels of ^7Li, with the assumption that no even-parity levels should appear up to a neutron energy of 2 MeV,[2),3)] so as to reproduce almost satisfactorily the (n,α) reaction and the elastic scattering cross sections of ^6Li below 20 MeV. In this work the calculated peak value of 3.01 barns at the $5/2^-$ resonance near 250 keV for the (n,α) reaction cross section was in good agreement with the bulk of recent measurements[4)-6)], but those of 8.83 barns for the elastic cross section and of 11.78 barns for the total cross section were slightly higher than experimental values. The measured values of them are 7.2 ± 0.4 barns by Lane et al.[7] and 11.0 ± 0.1 barns by Harvey and Hill,[8] respectively. This inconsistency at this resonance had been also found in the other works. Therefore, it was necessary for our study that the peak values should be reproduced self-consistently.

Recently Fort has corrected his (n,α) data.[4] The corrected peak value is 3.4 ± 0.2 barns.[9] In addition, the recent measurement of the (n,α) cross section by Gayther[10] has given a peak value of 3.29 ± 0.12 barns. On the other hand, recent experimental data of the elastic cross section by Knitter and Budtz-Jørgensen[11] are higher than the earlier values of Lane et al.[7] in the region of resonance, and Knitter's peak value of the total cross section is 11.20 ± 0.08 barns.

---

* Department of Nuclear Engineering, Osaka University

The partial widths Γ_n and Γ_α were re-estimated under the circumstances. The cross sections of the inelastic scattering to the 1st and the 2nd excited levels of ^{6}Li were also calculated, with the parameters determined through the fitting to experimental data of the (n,α) and the elastic cross sections, to inquire the reliability of the adopted parameters and the applicability of the approximations in our calculations.
The cross sections were calculated in terms of the Kapur-Peierls theory[12]. The total width Γ_ν, neutron width $\Gamma_{\nu n}$ and α-particle width $\Gamma_{\nu\alpha}$ were given by

$$\Gamma_\nu = \Gamma_{\nu n} + \Gamma_{\nu\alpha}, \quad \Gamma_{\nu n} = 2 \mid \delta_{\nu n} \mid^2 \sum_c P_c, \quad \Gamma_{\nu\alpha} = 2 \mid \delta_{\nu\alpha} \mid^2 \sum_c P_c.$$

Figs. 1 and 2 show the comparison of the present results with the experimental data of the (n,α) reaction and the elastic cross sections, respectively, in the energy range 0.01 - 20 MeV. The calculated curves by Holt et al., which are transcribed from the graphs in Ref. 13, lie far below the experimental points in the MeV region. The present results drawn by solid curves were obtained with the best fit values of the parameters listed in Table 1. The present calculation gave a peak (n,α) cross section of 3.28 barns at 240 keV, a peak elastic of 7.97 barns at 250 keV and a peak total of 11.20 barns at 250 keV. The calculated thermal values of the (n,α) and the elastic cross sections were 936 barns and 0.736 barns, respectively.

The cross secitons of ^{6}Li(n,n')^{6}Li(2.18 MeV) and ^{6}Li(3.56 MeV) were calculated with the parameter set shown in Table 1. The calculated values of the ^{6}Li(n,n')^{6}Li(3.56) cross section were about 20 times as high as the experimental values.

References

1) Komoda, S. and Igarasi, S. : JAERI-M 7148 (in Japanese) (1977).
2) Chesterfield, C.M. and Spicer, B.M. : Nucl. Phys. 41 675 (1963).

3) Aswad, A., Kissener, H.R., Jagur, H.U. and Eramzhian, R.A. : Nucl. Phys. A 208, 61 (1973)

4) Fort, E. and Marquette, J.P. : EANDC(E) 148 (1972).

5) Poenitz, W.P. : Z. Phys. 268, 359 (1974).

6) Coates, M.S., Hunt, G.J. and Uttley, C.A. : EANDC(UK)151, 10 (1974).

7) Lane, R.O., Langsdorf, A.S. Jr., Monahn, J.E. and Elwyn, A.J. : Adv. Phys. 12, 135 (1961).

8) Harvey, H.H. and Hill, N.W. : Proc. of 4th Conf. on Nuclear Cross Sections and Technology, Washington, 244 (1975).

9) Informed from Tsukada, K. as a report of the NEANDC Sub-committee on Standards and Discrepancies.

10) Gayther, D.B. : AERE-R 8556 (1977).

11) Knitter, H.H. and Budtz-Jϕrgensen, C. : Proc. of the 1976 International Conf. on the Interactions of Neutrons with Nuclei, Lowell, Paper PG2/I5 (1976).

12) Kapur, P.L. and Peierls, R.E. : Proc. Roy. Soc. (London) A166, 277 (1938).

13) Holt, R.J., Firk, F.W., Hickey, G.T. and Nath, R. : Nucl. Phys. A237, 111 (1975).

Table 1. The best fit values of parameters.

E_n (MeV)	J^{Π}	Γ_n (MeV)	Γ_α (MeV)	arg δ_n (radian)	arg δ_α (radian)
0.25	$5/2^-$	0.0577	0.0229	0	0
2.3	$1/2^+$	1.92	1.02	0	0
2.9	$3/2^-$	0.867	0	0	
4.1	$1/2^-$	0.943	0	0	
4.7	$3/2^-$	1.53	0	0	
4.7	$1/2^+$	6.06	0.44	0	0
7.6	$3/2^+$	5.23	0.98	-2.31	+0.78
9.3	$3/2^+$	6.35	1.68	-2.11	-0.96
12.8	$3/2^+$	6.86	2.28	-1.61	-1.59

Interaction radii ; a_n = 2.73 fm, a_α = 3.10 fm.

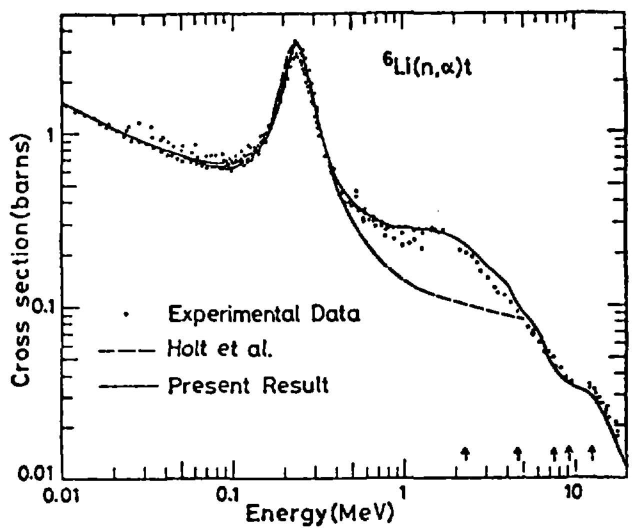

Fig. 1 Comparison of the present result for the ^{6}Li(n, α)t reaction cross section with experimental data and the calculated values by Holt et al.[10]. Five arrows show the locations of even-parity levels.

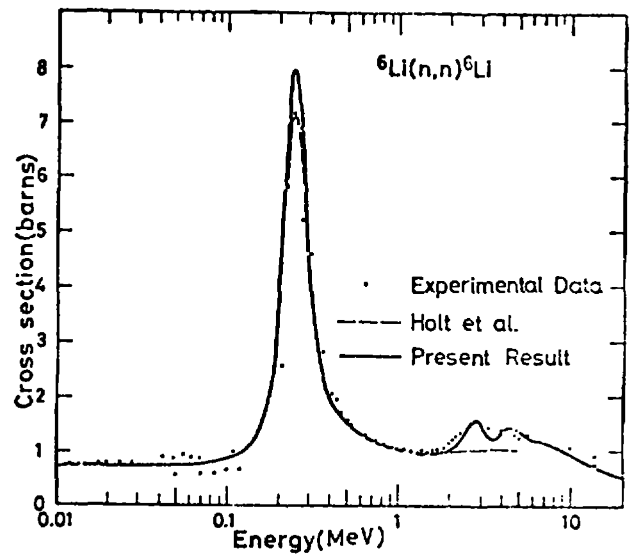

Fig. 2 Comparison of the present result for the elastic scattering cross section with experimental data and the calculated values by Holt et al.[10]. In the region of resonance, the earlier experimental data by Lane et al.[9] are shown.

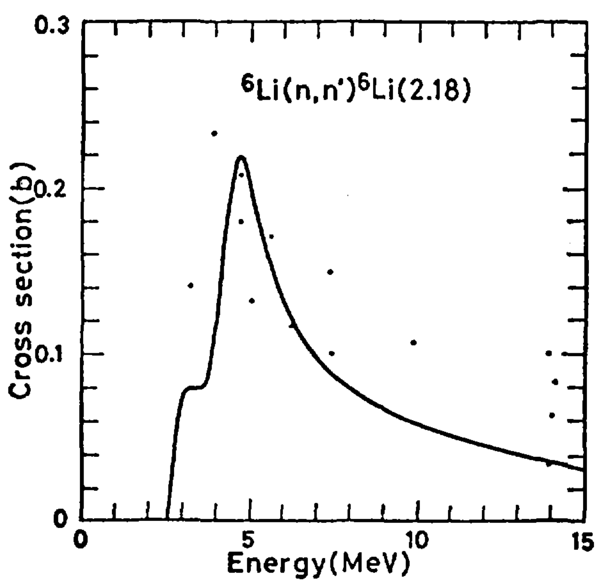

Fig. 3 Comparison of the present result with experimental data for the inelastic scattering to the 1st excit -ed level of ^{6}Li.

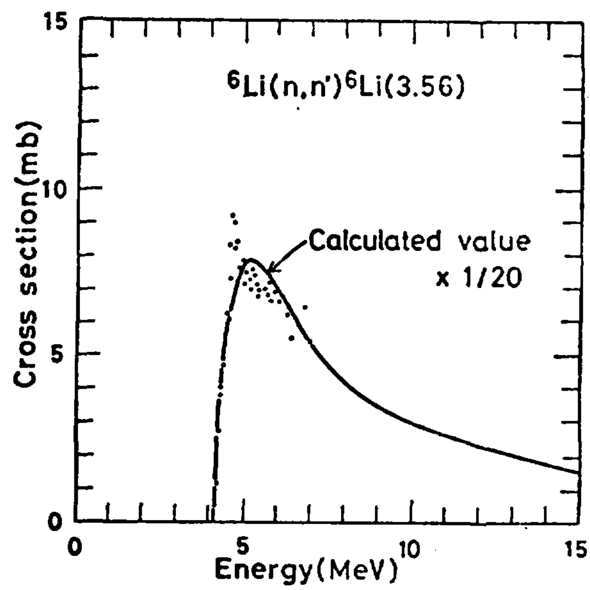

Fig. 4 Comparison of the present result with experimental data for the inelastic scattering to the 2nd excit -ed level of ^{6}Li.

II-C-2 Evaluation of Neutron Nuclear Data for ^{243}Am and ^{244}Cm.

S. Igarasi and T. Nakagawa

Evaluation of neutron nuclear data for ^{243}Am and ^{244}Cm below 16 MeV was performed. Selections of the resonance parameters were made below 250 eV for ^{243}Am and 1000 eV for ^{244}Cm, respectively, and the thermal values of the elastic scattering, capture and fission cross sections were obtained from the adopted resonance parameters. An average fission width for ^{243}Am was assumed in order to bridge the gap between the cross sections at thermal energy and those above 250 eV. Comparison of the results with the experimental data of thermal cross sections showed a good agreement for both nuclides.

Using a semi-empirical formula, the fission cross sections above the resonance region were investigated. The compound nucleus formation cross section in this formula was calculated from the optical model used in the previous work[1~3] for ^{241}Am. The other cross sections were obtained by using the statistical model codes. Number of the neutrons per fission was estimated from the experimental data and the empirical formula of Howerton.[4]

Since the tendency of the data of the fission cross section for ^{243}Am below 100 keV were very suspicious, an artificial modification was tried. However, no certain results could be obtained owing to the poor status of the experimental data. The present results above 100 eV are shown in figures with the other cross sections.

References :

1) S. Igarasi : JAERI-M 6221 (1975)

2) T. Nakagawa, T. Fuketa, and S. Igarasi : JAERI-M 6636 (1976)

3) S. Igarasi : J. Nucl. Sci. and Technol. 14, 1, (1977)

4) R.J. Howerton : Nucl. Sci. and Eng. 62, 438, (1977)

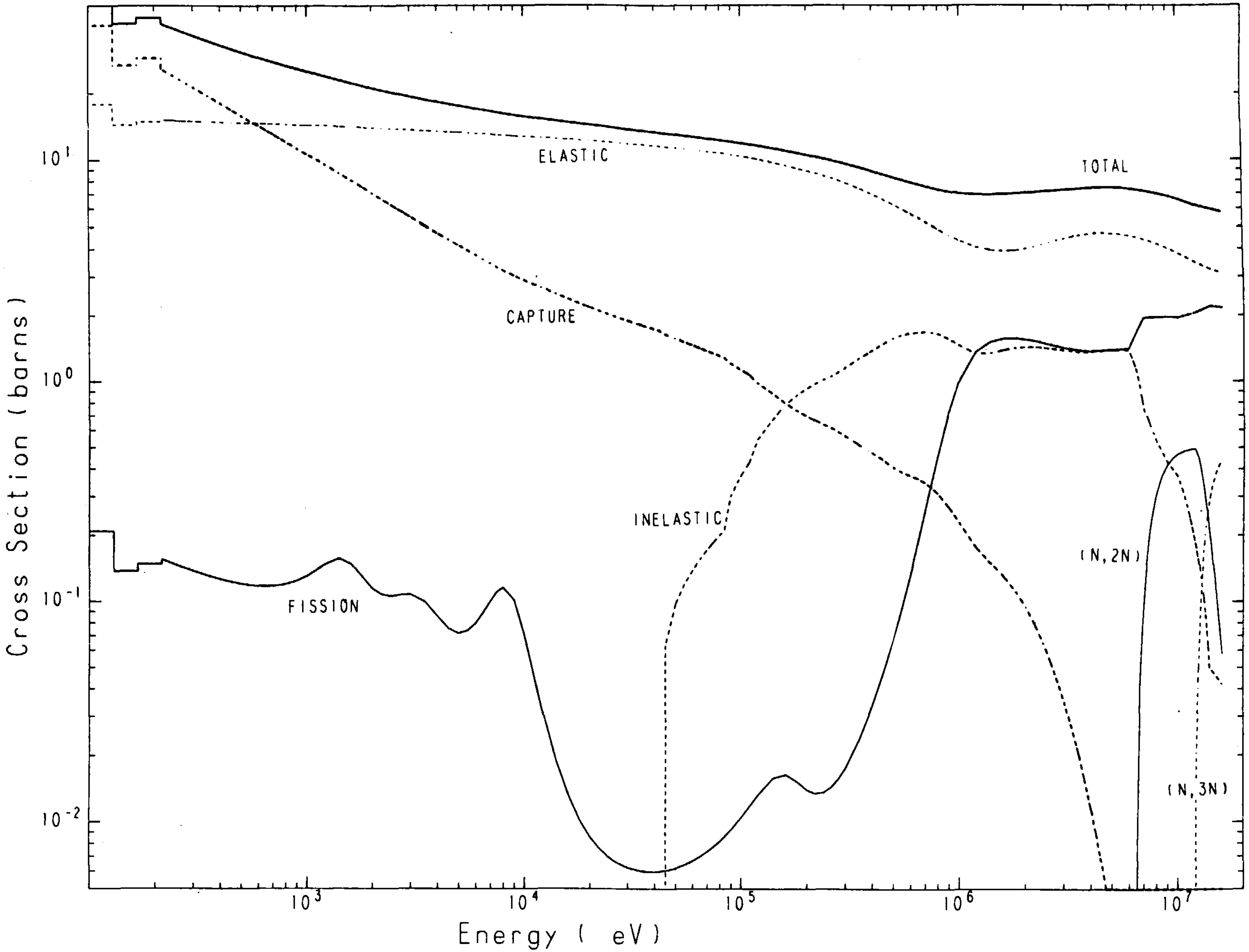

Cross sections of ^{243}Am above 100 eV.

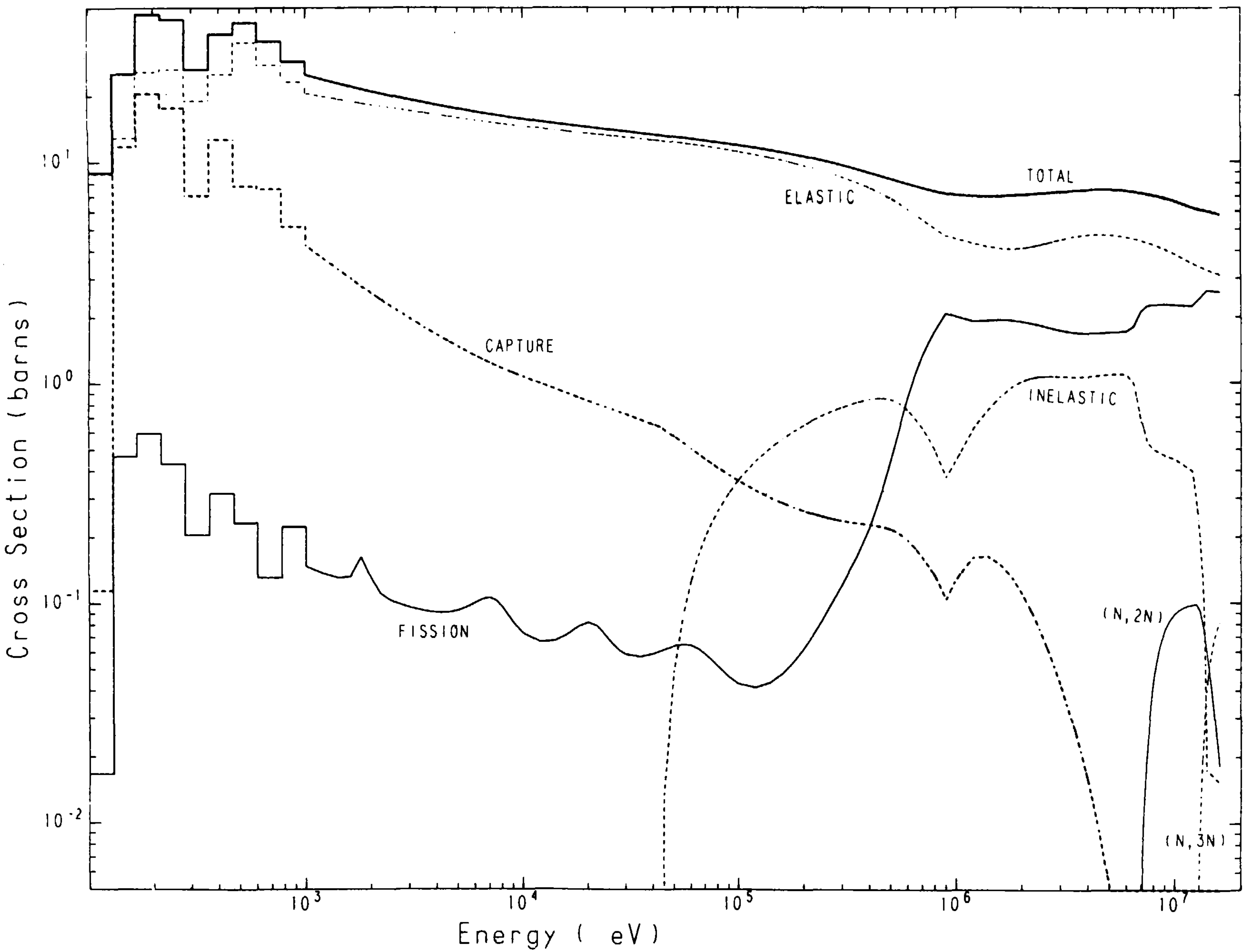

Cross sections of ^{244}Cm above 100 eV.

Test of FP Data in JENDL-1 by Using New Information on Integral Data

Y. Kikuchi and A. Hasegawa

Evaluation of neutron nuclear data was completed in 1973 by Japanese Nuclear Data Committee (JNDC) for 28 fission product (FP) nuclides[1), which are the most important for fast reactor, and the evaluated data are now stored in Japanese Evaluated Nuclear Data Library Version 1 (JENDL-1).

The multi-group constants were produced from these evaluated data, and the lumped group constants were provided. A system called JNDC FP Fast Reactor Constants System was developed for producing the lumped FP group constants automatically from JENDL-1 files. The reliability of the FP group constants was examined with the integral measurements made at the STEK facility in ECN, Petten, the Netherlands. The reactivity worths were calculated for three FP mixture samples and 22 FP isotope samples, and were compared with the experimental data. It was concluded that the constants based on JENDL-1 gave good agreement with the experiments both for FP mixtures and for FP isotopes. The details were given in JAERI-1248.[2)]

After publishing JAERI-1248, it was informed from ECN, Petten that the finally adopted values of the flux and the adjoint flux of STEK cores were changed a little from those used in the calculations in JAERI-1248. Therefore the calculations were made again by using the new flux and adjoint flux[3)]. The results are given here.

The central reactivity worths were calculated for two irradiated FP mixture samples, HFR-101 and HFR-102, and a mock-up sample (KFK-sample). The calculation was made by using the JENDL-1 constants set, which was called the JNDC set in JAERI-1248, the JNDC-P set, the Cook set and the ENDF/B-IV set. The results are given in Table 1. It was also informed[4)] that the HFR-102 sample and KFK-sample contained a considerable amount of moisture and therefore the experimental data reported in Ref. 5 must be modified. However, only small part of the modified values are available, and the C/E values are given in Table 1 only for the limited cases. It is evident from Table 1 that agreements between calculation and experiment are much improved with the new flux and adjoint flux. It can be also pointed out that the anomalons core dependence disapperars with the correction of moisture for KFK sample.

The reactivities of 22 FP isotopes were calculated with the new flux and adjoint flux. It was informed from ECN[6] that the self-shielding correction of the samples was very difficult and that the experimental data reported in Ref. 7 had a considerable error. However, the table of self-shielding factors was not yet provided for JENDL-1 constants and therefore we compared the results tentatively with the experimental data reported in Ref. 7. The C/E values are increased with the new flux and adjoint flux particularly for the core with hard spectrum. The C/E values are improved in STEK-500, 1000 and 2000 for most of cases except ^{104}Ru, ^{129}I and ^{144}Nd.

References

1) Iijima, S. et al. : J. Nucl. Sci. Technol., 14, 161 (1977)

2) Kikuchi, Y. et al. : "Fission Product Fast Reactor Constants System of JNDC", JAERI-1248 (1976)

3) Hoekstra, E.K. : "Fast Reactor Programme,Fourth Quarter 1976 Progress Report", ECN-15 (1977)

4) idem ; ibid, Combined Second and Third Quarters 1976 Progress Report, ECN-7 (1976)

5) Gruppellaar, H. et al. : "RCN-1 Pseudo Fission Product Capture Group Cross Sections", RCN-205 (1974)

6) Veenema, J.J., Janssen, A.J., : "Small Sample Reactivity Worths of Fission Product Isotopes and Some Other Materials Measured in STEK" ECN-10 (1976)

7) Hoekstra, E.K. : "Fast Reactor Programme, Second, Third and Fourth Quarter 1973 Progress Reports" RCN-190 (1973), RCN-199 (1973) and RCN-207 (1974)

Table 1. Comparison of capture components of the central reactivity worths $(-\rho/\rho_o)$ for FP mixtures

STEK Core	Sample	Exp	JENDL			JNDC-P			Cook			ENDF/B-IV		
			New Value	C/E New	C/E Old	New Value	C/E New	C/E Old	New Value	C/E New	C/E Old	New Value	C/E New	C/E Old
4000	HFR-101	0.501	0.5136	1.03	0.86	0.5852	1.16	1.0	0.4852	0.97	0.82	0.4796	0.96	0.79
	HFR-102		0.5507			0.6258			0.5205			0.5155		
	KFK	0.669	0.6570	0.98	0.81	0.7092	1.06	0.88	0.6192	0.93	0.76	0.6178	0.92	0.75
3000	HFR-101	0.406	0.4113	1.01	0.87	0.4988	1.23	1.06	0.3955	0.97	0.84	0.3684	0.91	0.78
	HFR-102		0.4339			0.5272			0.4180			0.3893		
	KFK		0.4912			0.5530			0.4612			0.4415		
2000	HFR-101	0.346	0.3587	1.04	0.89	0.4468	1.29	1.13	0.3495	1.01	0.87	0.3172	0.92	0.79
	HFR-102		0.3754			0.4698			0.3666			0.3323		
	KFK		0.4192			0.4815			0.3956			0.3720		
1000	HFR-101	0.287	0.2829	0.99	0.89	0.3579	1.25	1.12	0.2829	0.99	0.90	0.2511	0.87	0.89
	HFR-102	0.398	0.2937	0.74	0.67	0.3743	0.94	0.85	0.2941	0.74	0.67	0.2607	0.66	0.59
	KFK	0.339	0.3292	0.97	0.88	0.3825	1.12	1.02	0.3155	0.93	0.85	0.2933	0.87	0.79
500	HFR-101		0.1950			0.2421			0.2044			0.1781		
	HFR-102		0.2015			0.2519			0.2108			0.1838		
	KFK		0.2326			0.2666			0.2290			0.2114		

Benchmark Test of JENDL-1 File

A. Hasegawa and Y. Kikuchi

The Japanese Evaluated Nuclear Data Library Version 1 (JENDL-1)[1] has been developed by Nuclear Data Center, JAERI in cooperation with Japanese Nuclear Data Committee (JNDC), and is now open to use. For confirming its applicability before publishing, various benchmark tests were performed by "Working Group on Integral Tests for JENDL" in JNDC.

The multi-group cross section set was produced from JENDL-1 file by using the processing code system PROF-GROUCH-GII[2] and ETOX-II[3]. The group structure is the same as that of the JAERI-Fast Set[4] with 70 groups. The items of benchmark test were restricted to the central static characteristics of the core, as this test is the first step to assess the applicability of JENDL-1. A code system named "GC-EVACOS" was used, which performs benchmark test for specified items and statistical analysis of the results fully automatically.

Total of 21 assemblies were selected mainly from international benchmark cores and supplementary from FCA, MOZART and ZPR cores. Test items are, (1) effective multiplication factor, (2) central reaction rete ratio, (3) central reactivity worth and (4) Doppler reactivity coefficients. The last item was adopted for check of the selfshielding factors. The results obtained so far are shown in Table 1 ∿ 4 as the ratio of calculated value to experimental one (C/E value) together with the results from JAERI-Fast Set Version II R[5] and ENDF/B-IV[6]. In these tables, symbols A,B and C represent the following statistical values in each item respectively,

A : Statistical average : $\overline{(C/E)} = \sum_{i=1}^{N} (C/E)_i/N,$

B : Average of absolute difference from 1 :

$$\overline{|1.0 - C/E|} = \sum_{i=1}^{N} |1.0 - (C/E)_i|/N,$$

C : Standard deviation :

$$\text{St. Dev.} = \sqrt{\sum_{i=1}^{N} [(C/E)_i - (C/E)]^2/N}$$

(1) Effective multiplication factor

JENDL-1 gives the average value of 1.00294 for k_{eff} with 1.08% of standard deviation, while J.F.S. gives 0.999 and ENDF/B-IV 0.997. JENDL-1 overestimates average value of k_{eff} by 0.7% for U-fueled cores and also by 0.1% for Pu-fueled cores. Particularly in mirror reactors such as VERA-II-A vs. VERA-1-B and ZPR-6-6A vs. ZPR-6-7, disagreements of k_{eff} between U-fueled and Pu-fueled cores are evident. This may suggest that some inconsistencies still exist in the cross sections of ^{239}Pu and ^{235}U.

(2) Central reaction rate ratio

JENDL-1 gives satisfactory results for $^{238}U/^{235}U$ fission ratio, $^{240}Pu/^{235}U$ fission ratio and the ratio of the capture rate in ^{238}U to the fission rate in ^{235}U. On the other hand, rather poor results for $^{239}Pu/^{235}U$ fission ratio may also suggest the inconsistencies in the cross sections of ^{235}U and ^{239}Pu.

(3) Central Reactivity Worth

In the present analysis, both the calculated and experimental values are normalized to the reactivity of ^{239}Pu, in order to avoid the reactivity scaling problem.

From Tbale 3, it is suggested that some inconsistencies exist among the results of ^{239}Pu, ^{235}U and ^{238}U and that some drawbacks exist in the cross sections of Fe.

(4) Doppler reactivity coefficient

We analyzed zone Doppler experiments performed in SEFOR and small sample Doppler experiments performed in ZPPR, ZPR and FCA. The results obtained by JENDL-1 and J.F.S. show the two extremes. JENDL-1 overestimates the results by about 10%, and J.F.S. underestimates them by about 10%, though the calculated values remain within the limit of the experimental errors for both cases. This difference is mainly due to the differences in calculated spectrum in keV region.

Summarizing the results, it is concluded that JENDL-1 gives satisfactory results for the analyses of fast reactors. However some inconsistencies were pointed out for the cross sections of the primary fissionable nuclides such as ^{235}U, ^{238}U and ^{239}Pu and of the main structural material Fe.

References

1) Kikuchi, Y., et al. : JAERI-M-6996 (1977).

2) Hasegawa, A., et al. : to be published.

3) Wright, R. Q., et al. : ORNL-TM-2679 (1969).

4) Katsuragi, S., et al. : JAERI-1195 & 1199 (1970).

5) Takano, H. : to be published.

6) Hardie, R.W., et al. : Nucl. Sci. Eng., 57, 222 (1975).

Table 1. Effective multiplication factor. (K_{eff}) (C/E)

		JENDL-1	JFS VIIR	ENDF/B-IV
	A	1.00126	0.99747	——
Pu Fuel 15 cases	B	0.00697	0.00668	——
	C	0.01055	0.01230	——
	A	1.00714	1.00371	——
U Fuel 6 cases	B	0.01058	0.00864	——
	C	0.01036	0.00949	——
	A	1.00294	0.99926	0.9972
All 21 cases	B	0.00800	0.00724	0.0068
	C	0.01083	0.01190	——

Table 2. Central reaction rate ratio (C/E)

QUANTITY		JENDL-1	JFS VIIR	ENDF/B-IV
Fission Rate (^{238}U)	A	0.999	1.029	1.037
Fission Rate (^{235}U)	B	0.068	0.070	0.075
	C	0.076	0.081	——
Fission Rate (^{239}Pu)	A	0.969	0.981	0.989
Fission Rate (^{235}U)	B	0.044	0.033	0.031
	C	0.037	0.034	——
Fission Rate (^{240}Pu)	A	1.012	1.068	1.084
Fission Rate (^{235}U)	B	0.087	0.096	0.113
	C	0.110	0.106	——
Capture Rate (^{238}U)	A	0.984	0.982	0.974
Fission Rate (^{235}U)	B	0.027	0.027	0.043
	C	0.030	0.031	——
Capture Rate (^{238}U)	A	1.013	0.999	0.976
Fission Rate (^{239}Pu)	B	0.041	0.040	——
	C	0.046	0.045	——

Table 3. Central reactivity worth (C/E)*

NUCLIDE		JENDL-1	JFS VIIR	ENDF/B-IV
^{235}U	A	1.031	1.004	1.014
	B	0.051	0.041	0.042
	C	0.059	0.057	0.060
^{238}U	A	1.098	0.994	0.950
	B	0.134	0.102	0.116
	C	0.204	0.140	0.130
^{10}B	A	0.945	0.911	0.836
	B	0.090	0.102	0.165
	C	0.110	0.112	0.115
Cr	A	0.952	1.309	1.359
	B	0.113	0.125	0.359
	C	0.168	0.333	0.205
Fe	A	0.880	1.018	1.109
	B	0.128	0.109	1.175
	C	0.097	0.129	0.275
Ni	A	1.118	1.153	1.167
	B	0.154	0.153	0.191
	C	0.199	0.154	0.196

* Normalized to the worth of ^{239}Pu

Table 4. Doppler reactivity coefficient (C/E)

	Assembly	JENDL-1	JFS VIIR
Small Sample Doppler Experiment	FAC V-1	1.163	0.812
	V-2	1.038	0.736
	VI-1	1.152	0.934
	VI-2	1.049	0.893
	ZPPR-2 NORMAL	1.133	0.957
	NA-Voided	0.966	0.957
	ZPR-3-47	1.014	0.944
Zone Doppler Experiment	SEFOR	1.171	1.047

II-D-1 Independent Yield of ^{134}Cs in the Thermal Neutron Fission of ^{235}U

H. Umezawa, T. Suzuki, S. Ichikawa and T. Yamashita

Although ^{134}Cs is a shielded nuclide for the beta decay chain of fission products, it is generally formed in irradiated uranium samples from neutron capture on ^{133}Cs which is not shielded from its precursor. In the NSRR - Nuclear Safety Research Reactor of JAERI - , however, irradiation can be completed in a very short period of time, 4-5 milliseconds, so that the path of secondary formation of ^{134}Cs from fission-product ^{133}Cs is surely closed. For the purpose of determining the independent yield of ^{134}Cs in the thermal neutron fission of ^{235}U, cesium was chemically separated from an irradiated test-fuel-rod of NSRR and the intensity ratio of the 796-keV gamma ray of ^{134}Cs to the 662-keV gamma ray of ^{137}Cs was measured.

The rod contained 94 g of UO_2 whose enrichment was 10 %. The number of fissions occurred in the rod was estimated to be 2.50×10^{15} from the amount of ^{137}Cs produced. Gamma-ray spectrometry was carried out with a Ge(Li) detector having 18 % relative efficiency.

Results are shown in Table 1. Error quoted to our result gives the 95% confidence limit of the mean of measured values. Systematic errors due to half-lives, gamma-ray branching ratios and relative photopeak efficiencies used in the data analysis are at most 1 to 2 % as a whole. McHugh has reported the independent yield of ^{134}Cs obtained from one-hour irradiated uranium samples by means of mass spectrometry.[1] Agreement between the present result and that of McHugh is good within the limits of experimental errors.

Table 1. Independent yield of ^{134}Cs in the thermal neutron fission of ^{235}U

	$^{134}Cs/^{137}Cs$ atom ratio	Independent fission yield	Fractional chain yield
This work	$(1.25 \pm 0.20) \times 10^{-6}$	7.8×10^{-8} *	1.02×10^{-6} *
McHugh	$(1.45 \pm 0.10) \times 10^{-6}$	8.9×10^{-8} ** 9.1×10^{-8} *	1.11×10^{-6} ** 1.18×10^{-6} *

*) Calculated by taking 6.263% and 7.68% as the cumulative chain yields of ^{137}Cs and ^{134}Xe, respectively.[2]

**) Figurs given by McHugh taking 6.17% and 8.06% as the cumulative chain yields of ^{137}Cs and ^{134}Xe.

References:

(1) McHugh, J. A.: J. Inorg. Nucl. Chem., 28, 1787(1966)

(2) Meek, M. E., Rider, B. F.: NEDO-12154-1(1974)

E. Radioisotope and Nuclear Engineering School

II−E−1

Evaluation of Neutron Cross Sections for ^{19}F in the Energy Range from 100 keV to 20 MeV

T. Sugi and K. Nishimura

Results of the present evaluation are published to JAERI-M 7253. Fig. 1 shows the evaluated cross-section curves obtained in this report. The abstract of this study is as follows:

Fast neutron cross sections of ^{19}F were evaluated on the total, (n,n), (n,n'), (n,2n), (n,α), (n,p), (n,d), (n,t), (n,αn'), (n,n'α), (n,pn'), (n,n'p) and (n,γ) reactions. Evaluated cross-section curves are presented in garphs together with the experimental data; evaluated cross-section data are given in tables. These evaluated cross-section curves were obtained in principle on the basis of the experimental data. In the following, these curves were calculated by using theoretical models. The total neutron cross section above 8.5 MeV was determined by an optical-model curve fitted to the experimental data. In the energy range from 1.0 to 5.5 MeV the (n,n') cross sections for the 1st to the 6th level were calculated by Hauser-Feshbach method in which the (n,α) and (n,p) reactions were taken into account as competitive processes. Above 5.5 MeV, the total inelastic scattering cross section was obtained by subtraction of all constituent cross sections other than inelastic from the non-elastic scattering cross section calculated by Hauser-Feshbach formula. The (n,d) and (n,t) cross sections were determined by using an empirical formula of Pearlstein. The (n,α) and (n,p) cross sections above 9 MeV and the cross sections for the (n,αn'), (n,n'α), (n,pn') and (n,n'p) reactions were calculated by using a statistical model in which Pearlstein's empirical formula was employed. The (n,2n) cross section was obtained by fitting Pearlstein's function of statistical model to the experimental data.

The (n,γ) cross section above 1.9 MeV was obtained by assuming a $1/v$ law. The elastic scattering cross section was finally obtained by subtracting all the evaluated partial cross sections from the total neutron cross section evaluated.

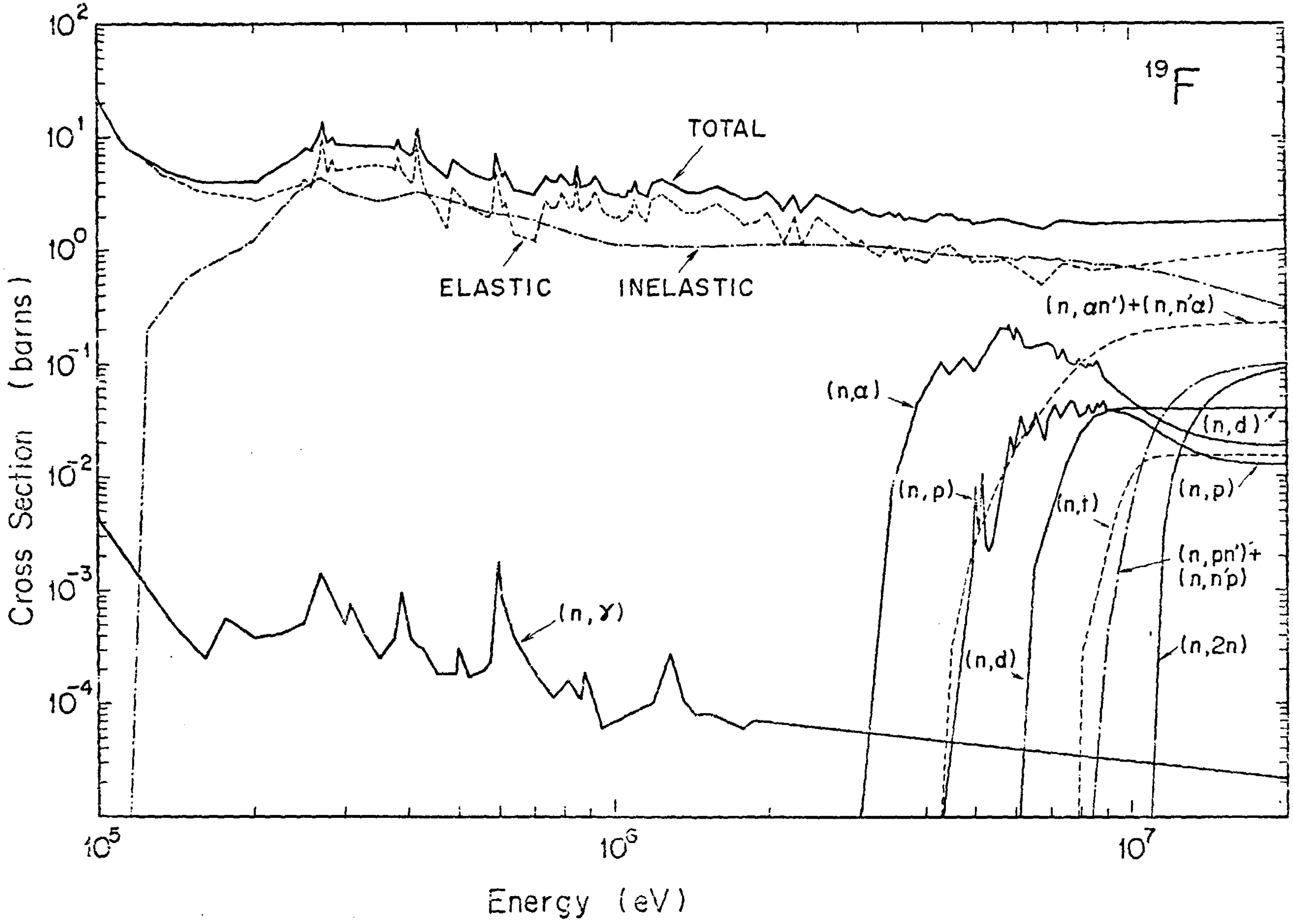

Fig. 1 The present result of the evaluated neutron cross sections for ^{19}F

III. KYOTO UNIVERSITY

A. Institute of Atomic Energy

III-A-1 Independent Fission-Yields of Several Iodine Isotopes in the Thermal-Neutron Induced Fission of ^{233}U, ^{235}U and ^{239}Pu

Tomota Nishi, Ichiro Fujiwara and Nobutsugu Imanishi

The independent fission yields of ^{131}I, $^{132}I^{m,g}$, ^{133}I and $^{134}I^{m,g}$ in the thermal-neutron fission of ^{233}U, ^{235}U and ^{239}Pu were measured by the radiochemical method.

Irradiation: A dilute nitrate solution containing 100 μg of ^{233}U, ^{235}U or ^{239}Pu was irradiated for 30 sec in the pneumatic transport system of the Kyoto University Reactor.

Chemical separation: The iodine samples were isolated from other fission products in a few minutes by a procedure proposed by Glendenin and Metcalf[1].

γ-ray measurement: γ-rays emitted from the samples were measured with a Ge(Li) detector.

Fission monitor: The activity of ^{135}I was used as the fission-yield monitor.

Determination of the independent yields: For the determination of the independent fission-yields, the measured activities were corrected for the contribution of those ones built up from the precursors during the irradiation and before the time of chemical separation.

Results: The results of the independent fission-yields are presented in Table 1. The errors include uncertainties of half-lives, absolute abundances of γ-rays, counting efficiencies, and fission-yields of the fission monitor and the precursors, in addition to the statistical errors in the activity measurements.

Table 1. Independent fission-yields

Chain	Independent yield (%)		
	I(total)	I(8^- state)	I(4^+ state)
^{233}U - 135	4.9 ± 0.2[a]	-	-
- 131	0.018 ± 0.004	-	-
- 132	0.19 ± 0.01	0.08 ± 0.01	0.11 ± 0.01
- 133	0.72 ± 0.05	-	-
- 134	1.79 ± 0.07	0.77 ± 0.04	1.02 ± 0.06
^{235}U - 135	6.3 ± 0.2[a]	-	-
- 131	0.0023 ± 0.0007	-	-
- 132	0.022 ± 0.002	0.010 ± 0.001	0.012 ± 0.002
- 133	0.12 ± 0.01	-	-
- 134	0.67 ± 0.06	0.31 ± 0.02	0.36 ± 0.02
^{239}Pu - 135	6.3 ± 0.2[b]	-	-
- 132	0.23 ± 0.01	0.11 ± 0.01	0.12 ± 0.01
- 133	0.94 ± 0.07	-	-
- 134	2.34 ± 0.08	1.10 ± 0.06	1.24 ± 0.06

a) Cumulative yield. Ref. 2)

b) Cumulative yield. Ref. 3)

References:

1) L.E.Glendenin and R.P.Metcalf, Radiochem. Studies: The fission products (ed. by C.D.Coryell and N.Sugarman), McGraw Hill, p.1625 (1951)
2) S.Amiel and H.Feldstein, Phys. Rev. C11, 845 (1975)
3) R.C.Hawking, W.J.Edwards and W.J.Olmstead, Can. J. Phys. 49, 785 (1971)

III−B−1

MEASUREMENTS OF NEUTRON TOTAL CROSS SECTION MINIMA IN NATURAL IRON AND SILICON

Katsuhei Kobayashi, Yoshiaki Fujita and Yoshihiro Ogawa

A paper on this subject was submitted to Annals of Nuclear Energy.

Neutron transmission measurements in thick natural iron and silicon samples were carried out by the linac time-of-flight method to obtain their cross section minima near 24 keV, and 147 keV, respectively. Their minima are shown in Fig. 1 and Fig. 2. The value of the cross section minimum for iron was 0.400 ± 0.02 barns at 24.3 ± 0.1 keV. The minimum value for silicon was 0.093 ± 0.004 barns at 147 ± 1 keV. Sharp minimum dip in the silicon cross section was also found at 54.5 ± 0.3 keV, and the minimum value was 0.14 ± 0.04 barns. ENDF/B-IV data for the iron cross section minimum agree with the present measurement, but they show serious disagreement with the present minimum values near the 55 and 147 keV for silicon.

References :

1) F. Rahn, H. Camarda, G. Hacken, W. W. Havens,Jr., H. I. Liou, J. Rainwater, M. Slagowitz and S. Wynchank, Nucl. Sci. Eng., 47 (1972) 372.

2) K. A. Alfieri, R. C. Block and P. J. Turinsky, Nucl. Sci. Eng., 51 (1973) 25.

3) D. I. Garber and R. R. Kinsey, "Neutron Cross Sections, Curves", BNL-325 3rd ed., Vol. II (1976).

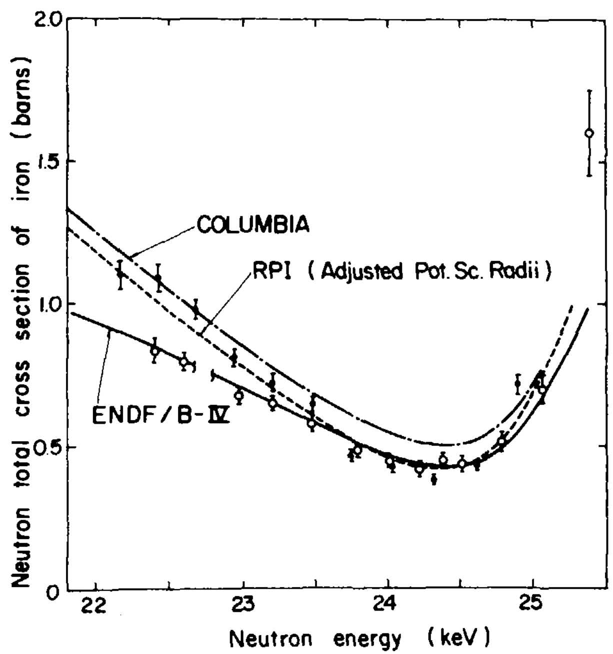

Fig. 1 Neutron total cross section of natural iron near 24 keV minimum,

ENDF/B-IV

Columbia data[1)]

RPI-result(Adjusted Pot. Sc. Radii) 2)

RPI experimental data[2)]

Present work .

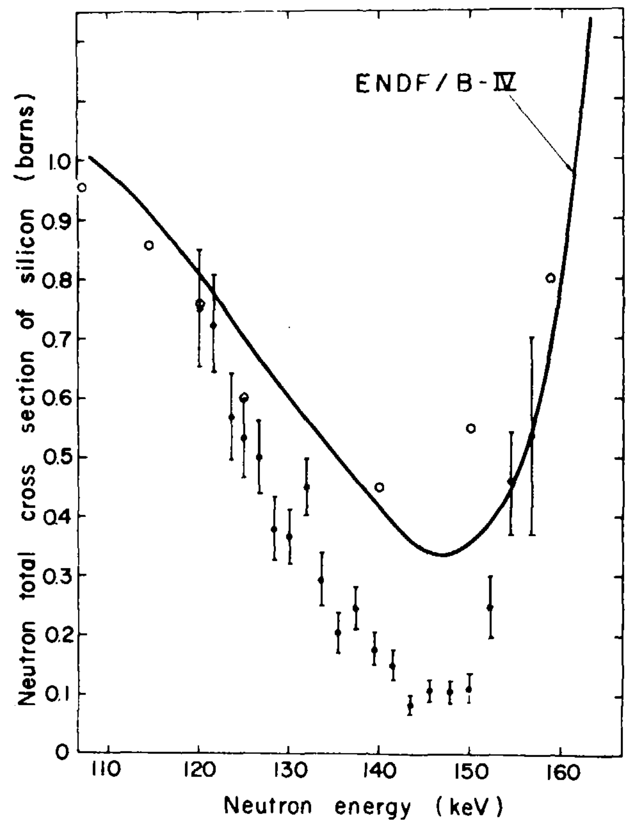

Fig. 2 Neutron total cross section of silicon near 147 keV minimum,

ENDF/B-IV

Data cited from BNL-325 3rd ed. (1976) 3)

Present work .

III-B-2

Measurements of Neutron Capture Cross Sections of U-238 and Cs-133 using Silicon-filtered Neutrons

Y.Fujita, K.Kobayashi, Y.Namioka, M.Igashira* and N.Yamamuro*

Iron and silicon filters provide the monoenergetic neutrons near 24 keV and 146 keV, respectively. The 24 keV iron-filtered neutrons were successfully used for the measurements of "point values" of total and capture cross sections[1)2)]. Main advantages of the neutron filtered beam technique are the reliable background subtraction and the ease of experimental set-up.

Measurements of neutron capture cross sections of U-238 and Cs-133 have been carried out by the linac time-of-flight method near 146 keV using silicon-filtered neutrons. The experiments were carried out at the 11.7 m TOF station of the KUR-linac facility using an iron filter of 20 cm thick and a silicon filter of 80 cm thick. Capture events were counted by detecting the associated prompt gamma-rays with C_6F_6 and C_6D_6 neutron-insensitive gamma-ray detectors[3)]. The cross sections near 146 keV are deduced from the following relations :

$$Y_X(146) = \frac{C_X(146)\cdot C_B(24)}{C_B(146)\ C_X(24)} \times \frac{Y_X(24)\ Y_B(146)}{Y_B(24)}$$

where

---

* Tokyo Institute of Technology

$Y_X(E)$: Capture or (n,$\alpha\gamma$) yield for sample X and E keV neutrons

$C_X(E)$: Measured count rate for sample X and E keV neutrons.

The reference cross sections were taken from the ^{10}B (n,$\alpha\gamma$) cross section[4] and the 24 keV values of the respective elements.[2] The time of flight spectra are shown in Fig.1 for B-10 and U-238 samples in the case of the silicon filter. As seen in Fig.1, the flight-time-seperated neutrons are obtained near 55 keV as well as 146 keV. The 55 keV neutrons are also used to determine the capture cross section near 55 keV. Preliminary results are presented in Table 1 along with the reference values and the values of ENDF/B-IV and Iijima et al.'s evaluation.[5]

References :

1) R.C.Block, et al. : J.Nucl.Sci.Technol., 12 , 1 (1975).
2) N.Yamamuro, et al. : Proc.of Conf.on Nucl.Cross Sections and Technol., NBS SP 425, p.802 (1975).
3) N.Yamamuro, et al. : Nucl.Instr.Meth., 133 , 531 (1976).
4) M.G.Sowerby, et al. : AERE-R-6316 (1970).
5) S.Iijima, et al. : J.Nucl.Sci.Technol., 14 , 16 (1977).

Table 1 Preliminary results of neutron capture cross section meaurements of U-238 and Cs-133 at 146 keV and 55 keV.

Element	U-238	U-238	Cs-133	Cs-133
Reference values at 24 keV (b)	0.50±0.035	0.50±0.035	0.58±0.034	0.58±0.034
Neutron energy (keV)	146	55	146	55
Present result (b)	0.187±0.017	0.34±0.05	0.21±0.017	0.37±0.033
ENDF/B-IV (b)	0.16	0.31	0.22	0.43
Iijima et al.(b)			0.20	0.36

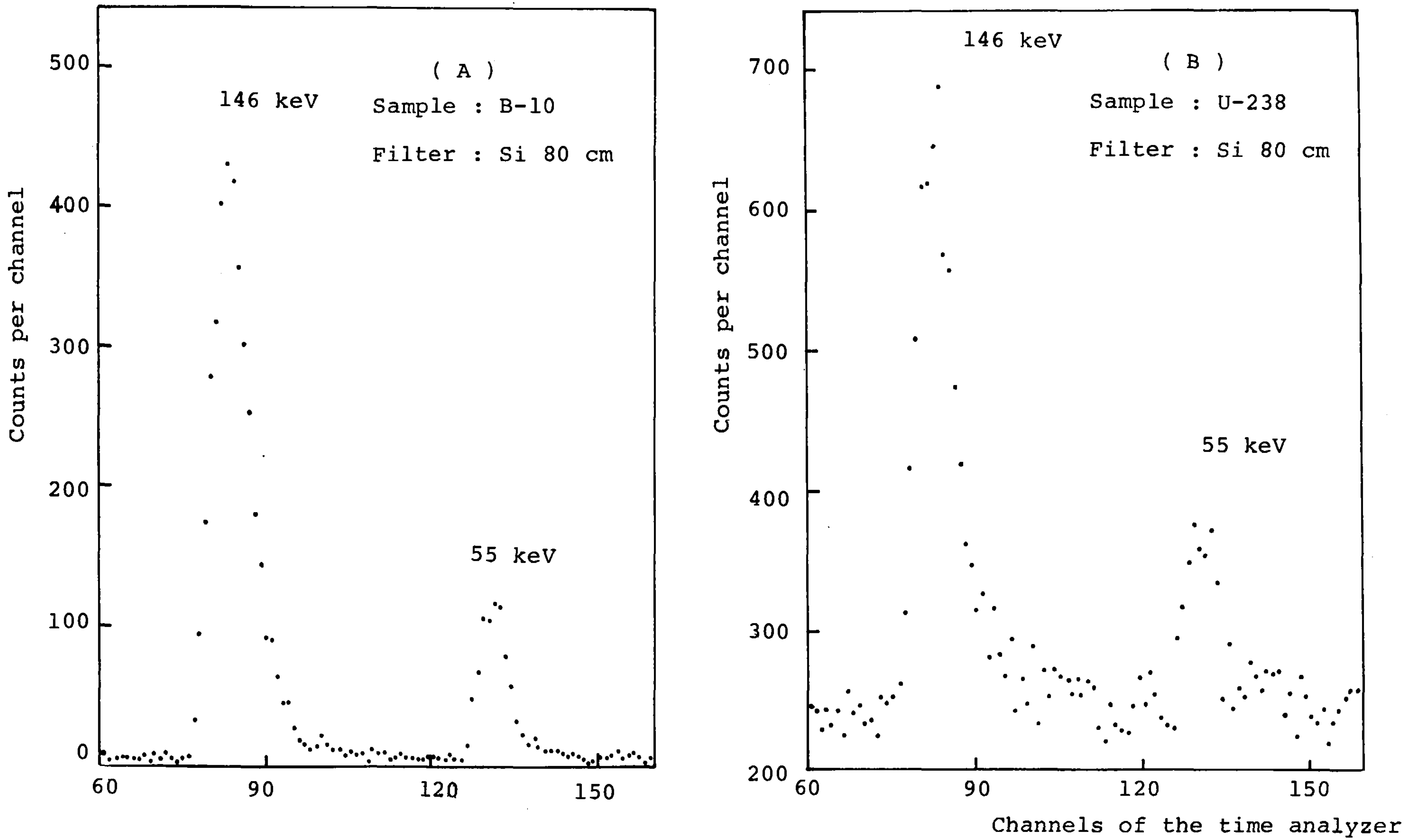

Fig. 1 Time of flight spectra for B-10 (A) and U-238 (B) in the case of the silicon filter.

III-B-3 FISSION SPECTRUM AVERAGED CROSS SECTION FOR THE ^{232}Th(n,f) REACTION

Katsuhei Kobayashi

A paper on this subject was published in Annals of Nuclear Energy, 4 (1977) 177-181.

Fission spectrum averaged cross sections for the ^{232}Th(n,f) reaction were measured relative to the average cross section of 102 mb for the ^{58}Ni(n,p)^{58}Co reaction, (1) at the beam port E-3 of the Kyoto University Reactor (KUR) where the fast neutron spectrum had previously been confirmed to be equivalent to that of fission neutrons[1), and (2) with a fission plate[2) installed at the thermal neutron facility of KUR. In the first experiment, a fission chamber composed of a thorium film and a silicon detector was used and the measured value was 77.4 $\pm$ 3.7 mb. Anisotropic effect in the fragment angular distributions was investigated by a Monte Carlo calculation. In the second experiment with the fission plate, induced-activities of ^{140}Ba in the thorium foil were measured with a Ge(Li) detector, and the result was 78.1 $\pm$ 3.9 mb. These data are in good agreement with each other. Most of the average cross sections calculated by several researchers are generally around 70 mb, which is smaller by about 10 % than the results of the integral measurements. The Fabry's value[3) is about 7 % larger than those of the author's.

References :

1) I. Kimura, K. Kobayashi and T. Shibata, J. Nucl. Sci. Technol., 8 (1971) 59.

2) K. Kanda, K. Kobayashi, H. Chatani and T. Shibata, KURRI-TR-96 (1972).

3) A. Fabry, BLG-465 (1972).

III-B-4 FISSION SPECTRUM AVERAGED CROSS SECTION FOR THE $^{231}Pa(n,f)$ REACTION

Katsuhei Kobayashi and Itsuro Kimura

A paper on this subject was submitted to Annu. Rep. Res. Reactor Inst., Kyoto Univ.

Fission spectrum averaged cross section for the $^{231}Pa(n,f)$ reaction has been measured relative to the average cross section of 1323 mb for the $^{237}Np(n,f)$ reaction. The cross section values measured with a fission plate installed at the thermal neutron facility of the Kyoto University Reactor (KUR) and in the core of KUR are shown in Table 1. In order to assess the energy dependent cross section for the $^{231}Pa(n,f)$ reaction, as shown in Fig. 1, average cross section calculated with the Maxwellian-type fission neutron spectrum was compared with the measurement. In this evaluation, the previous data by the authors[1)2)] have been taken in the energy region above about 3 MeV. The value calculated with the Muir's data[3)] below 3 MeV is in agreement with the measurement within an experimental error, while those by Williams[4)] below 3 MeV and by Drake and Nichols[5)] are about 21 % and 15 % lower than the measurement, respectively. The calculated with the Dubrovina's[6)] is rather close to the measurement.

Table 1 Fission spectrum averaged cross section for the $^{231}Pa(n,f)$ reaction

Cross section (mb)	Reference
1087 ± 68	Measured with the fission plate
1059 ± 76	Measured in the core of KUR
1037	Calculated with the energy dependent cross section by Muir[3] and the authors[1)2)] and the Maxwellian-type fission spectrum*
979	Calculated with the energy dependent cross section by Dubrovina[6] and the authors[1)2)] and the Maxwellian-type fission spectrum*
857	Calculated with the energy dependent cross section by Williams[4] and the authors[1)2)] and the Maxwellian-type fission spectrum*
927	Calculated with the energy dependent cross section by Drake[5] and the Maxwellian-type fission spectrum*

* $\overline{T}$ = 1.31 MeV, $\overline{E}$ = 1.97 MeV

References :

1) K. Kobayashi, I. Kimura, H. Gotoh and H. Yagi, Annu. Rep. Res. Reactor Inst., Kyoto Univ., 8 (1975) 10.

2) K. Kobayashi and S. Yamamoto, unpublished.

3) D. W. Muir, L. R. Veseer, CONF-710301, 3rd Conf. on Neutron Cross Sections and Technol., at Knoxville, Vol. I (1971) 292.

4) J. H. Williams, LA-150 (1944).

5) M. K. Drake, P. F. Nichols, GA-7462 (1967).

6) S. M. Dubrovina, V. A. Shigin, Doklady Akad. Nauk, SSSR-157 (1964) 561.

7) R. H. Iyer, M. L. Sagu, R. Sampathkumer, BARC 628 (1972) 94.

Fig. 1 Energy dependent cross section for the ^{231}Pa(n,f) reaction,

Kobayashi et al.[1)]

Kobayashi and Yamamoto[2)]

Muir et al.[3)]

Williams[4)]

Drake et al.[5)]

Dubrovina et al.[6)]

Iyer et al.[7)]

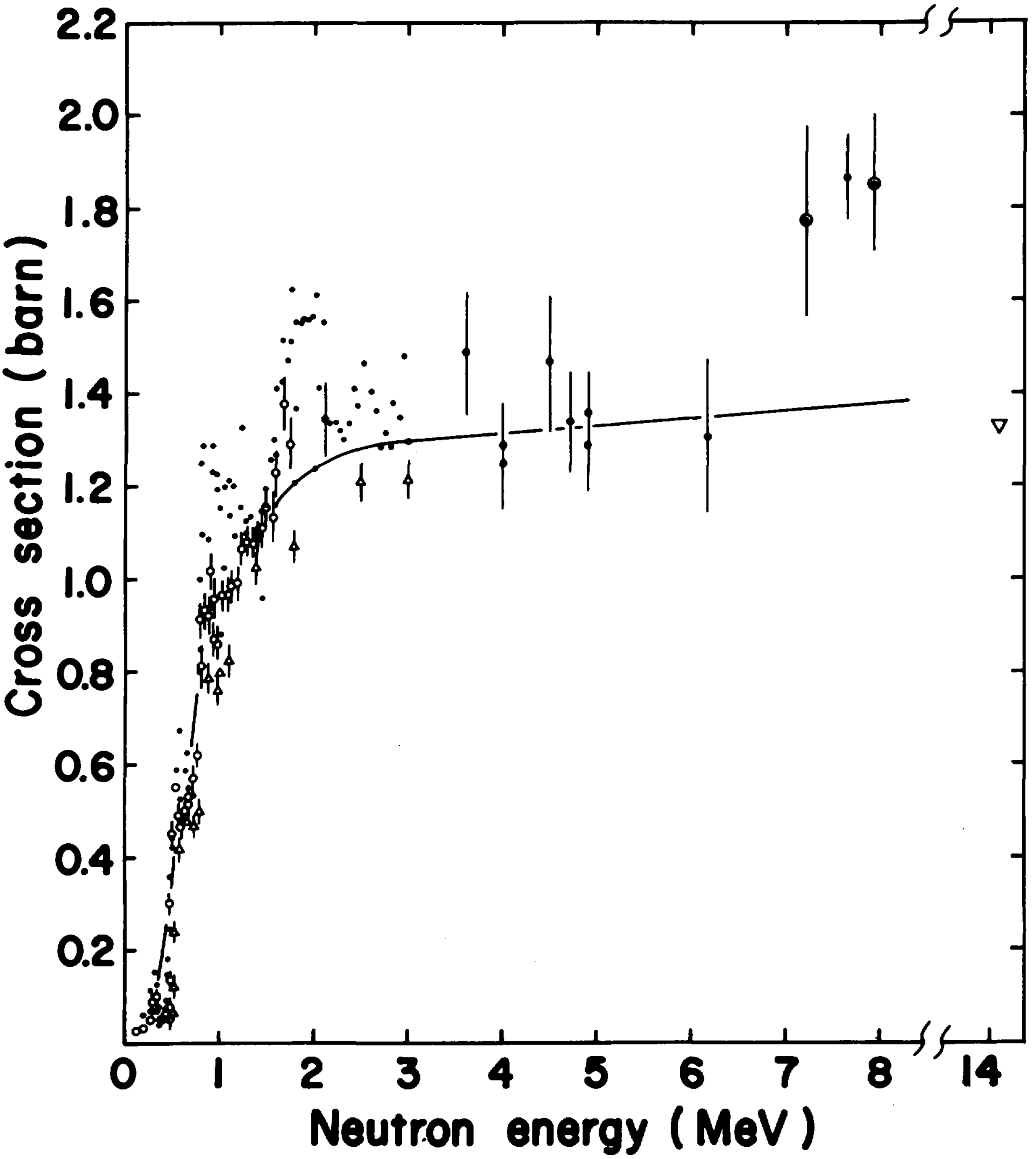

2.2
2.0
1.8
1.6
1.4
1.2
1.0
0.8
0.6
0.4
0.2
Cross section (barn)
0
1
2
3
4
5
6
7
8
14
Neutron energy (MeV)

III-B-5 Measurement and Analysis of Neutron Spectrum in Lithium Fluoride

Shu A. Hayashi, Itsuro Kimura, Katsuhei Kobayashi,
Shuji Yamamoto, Hiroshi Nishihara*, Satoshi Kanazawa*
and Masayuki Nakagawa**

In order to assess the nuclear data or group constants of lithium and fluorine, neutron spectrum in lithium fluoride pile of 60 cm in diameter was measured by the time-of-flight method using an electron linear accelerator as a pulsed neutron source.

The measured neutron spectra have been compared with the calculated one using the group constant produced from ENDF/B-IV. The results are shown in Fig. 1. It can be seen that the measured spectra in the lithium fluoride pile (r=15 cm, μ=0.0) generally agrees with one predicted by the theoretical calculation except a dip around 50 keV.

---

* Department of Nuclear Engineering, Kyoto University, Yoshida-honmachi, Sakyo-ku, Kyoto

** Japan Atomic Energy Research Institute, Tokai-mura, Ibaraki

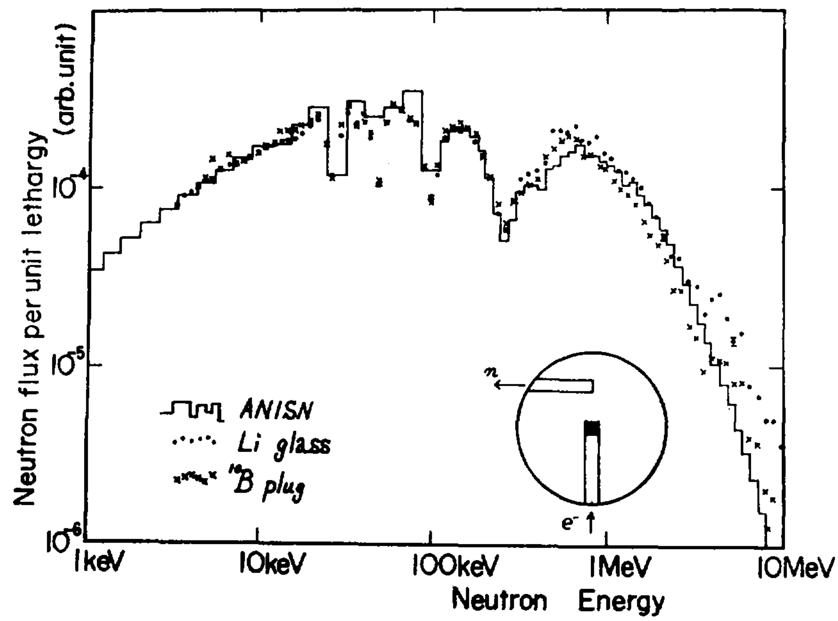

Fig. 1 Neutron spectrum in a lithium fluoride pile

(r=15 cm, μ=0.0).

Experimental/ ^{6}Li glass scintillation counter

Experimental/ ^{10}B-vaseline-NaI(Tl) counter

Calculated/ ANISN,ENDF/B-IV

III-B-6 Half-Lives and Gamma-Ray Energies of Short-Lived Molybdenum Isotopes

Y. Kiso*, R. Matsushita, J. Takada, H. Takemi* and T. Tamai

A paper on this subject was published in J. Nucl. Sci. Technol., 14[7], 482 (1977).

Short-lived molybdenum isotopes produced by the ^{235}U (n, f) reaction were isolated by rapid paper electrophoretic technique. The objectives of the present work are (a) to examine the discrepancies prevailing among the reported half-lives of ^{103}Mo, ^{104}Mo and ^{105}Mo, by tracing the genetic relationships of their technetium daughters, and (b) to identify the γ -rays emitted from $^{103\text{-}105}Mo$.

Several microliters of 0.01 M $UO_2(CH_3COO)_2$ embodying ^{235}U enriched to 90% were irradiated in sealed polyethlene capillary tube under a thermal neutron flux of 2.35×10^{13} n/cm^2 sec for 10 sec in a pneumatic tube of the Kyoto University Reactor. The electrophoretic separation is started about 15 sec after the end of irradiation, under a potential gradient of 5,000 V/ 10 cm, to last 20 sec. Gamma-ray measurement of the isolated molybdenum fraction is commenced 5 sec after the end of the separation and repeated during 500 sec at intervals of 20 sec counting time plus 2.5 sec recording time. The 44 data of γ -spectra thus obtained successively were accumulated to reduce the statistical error.

---

* Faculty of Engineering, Hiroshima University, Hiroshima

The half-lives of ^{103}Mo (70±1 sec), ^{104}Mo (66±2 sec) and ^{105}Mo (30±3 and 40±5 sec) were determined by analyzing the genetic relationships of the known photopeaks of their technetium daughters. Decay analysis of observed photopeaks free from interference resulted in the detection of many new short-lived photopeaks with half-lives of 10-70 sec, and which were ascribed to $^{103-106}Mo$, based on examination of their decay behavior.

IV. KYUSHU UNIVERSITY

Department of Nuclear Engineering, Faculty of Engineering

IV-1 Precompound Processes in Inelastic Scattering of 14.1 MeV Neutrons by Cu, As, Nb and Ag

Y. Irie, M. Hyakutake, M. Matoba,
I. Kumabe and M. Sonoda

This work was completed and a full paper has been published in Memoirs of the Faculty of Engineering, Kyushu University, Vol. 37 (1977) 19 with an abstract as follows ;

Energy and angular distributions for inelastic scattering of 14.1 MeV neutrons from Cu, As, Nb and Ag were measured by time-of-flight method. Angle-integrated energy spectra were analysed by both the compound and precompound models and the best-fit values were obtained for the model parameters related to the absolute inelastic scattering cross section. The Exciton and the geometry dependent hybrid models were used for the precompound model calculation. It was found that the geometry dependent hybrid model can reproduce well the experimental cross sections when the average values of the best-fit parameters are used. Angular distributions of neutrons from the precompound decay were calculated by a simple analytical method in terms of surface interaction. A general trend of the experimental results was reasonably well reproduced.

IV-2 Analysis of the Total (n,p) and (n,α) Cross Sections at 14 MeV with the Pre-Equilibrium Model

I. Kumabe, M. Hyakutake and Y. Fujino

Levkovskii[1] has critically evaluated the reliability of all the published data and has presented the most reliable averaged values of the (n,p) and (n,α) cross sections at 14 MeV.

The values after the subtraction of the calculated (n,p) cross section based on the statistical evaporation model from the experimental ones evaluated by Levkovskii were compared with the calculated values based on the pre-equilibrium model. The ratios of the experimental to calculated cross sections $\sigma_{exp}/\sigma_{cal}$ are plotted in the middle part of Fig. 1. We found the strong correlation between $\sigma_{exp}/\sigma_{cal}$ and $a/\bar{a}$, where a is the level density parameter and $\bar{a}$ the mean level density parameter which is equal to A/7.5. Thus the correction of $(a/\bar{a})^2$ to σ_{cal} was carried out. The values of $(\sigma_{exp}/\sigma_{cal})/(a/\bar{a})^2$ are plotted in the lower part of Fig. 1. The deviation of the points from 1.0 are successfully reduced. In the case of the (n,α) reaction, we also found the strong correlation between $\sigma_{exp}/\sigma_{cal}$ and $a/\bar{a}$. Thus the calculated (n,α) cross sections corrected by a function of a are expected to reproduce the experimental ones without the use of unknown parameter φ which is collision probability between the incoming particle and an α-cluster preformed in the nucleus.

Reference :

1) V. N. Levkovskii : Sov. J. Nucl. Phys. 18 (1974) 361.

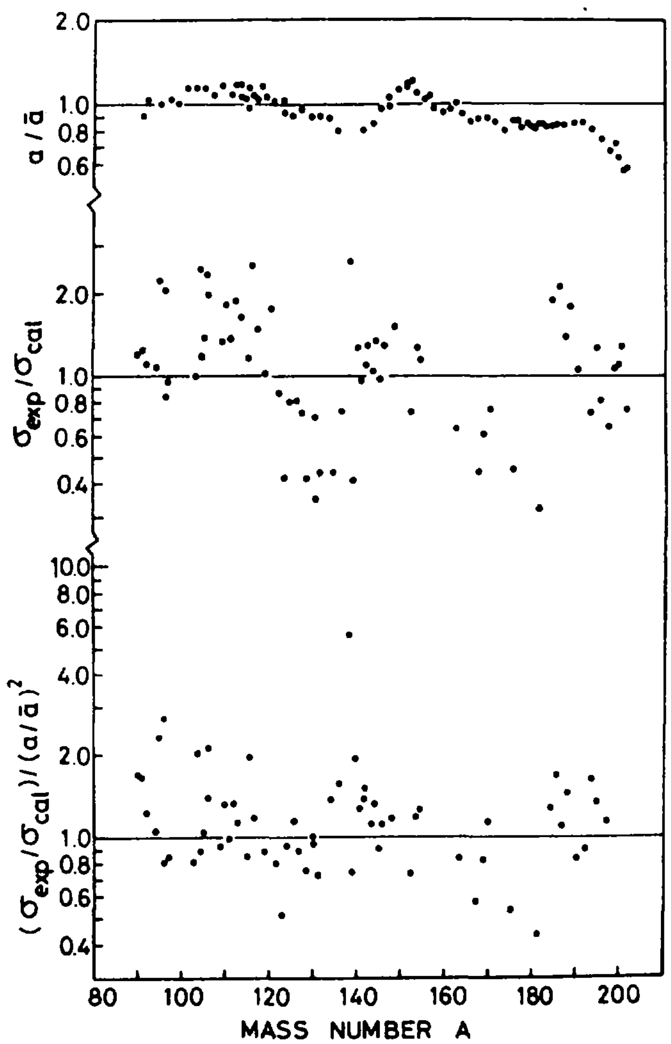

Fig. 1 The ratios of the level density parameter to the mean level density parameter $a/\bar{a}$, the ratios of the experimental to calculated cross sections $\sigma_{exp}/\sigma_{cal}$, and the values of $(\sigma_{exp}/\sigma_{cal})/(a/\bar{a})^2$ plotted in the upper, middle and lower parts, respectively, versus the mass number.

IV−3 **Analysis of (n,2n) Cross Sections at 14.7 MeV in the Rare-Earth Region**

I. Kumabe

A paper on this subject was published in the Journal of Nuclear Science and Technology, 14 (1977) 460.

Qaim[1] has measured the cross sections for (n,2n) reactions at 14.7 MeV on 29 nuclides in the rare-earth region by the activation technique using Ge(Li) detector γ-ray spectroscopy. These systematic (n,2n) cross sections are compared with the theoretical calculations performed by a new model[2] including pre-equilibrium and statistical models. Most of the calculated (n,2n) cross sections agree with the experimental ones within the experimental errors. The mean value of $\sigma_{exp}/\sigma_{cal}$ is 1.003.

References :

1) S. M. Qaim : Nucl. Phys. A224 (1974) 319.

2) I. Kumabe, E. Kotake and F. Nagahama : J. Nucl. Sci. Technol. 14 (1977) 319.

IV−4 Activation Cross Sections on Zirconium and Molybdenum Isotopes Induced by 14.6 MeV Neutrons

Y. Fujino, M. Hyakutake and I. Kumabe

Activation cross sections for the (n,p), (n,α) and (n,2n) reactions on Zr and Mo isotopes have been measured at 14.6 MeV by using a Ge(Li) γ-ray detector. Table 1 shows the results obtained from the present work.

Table 1. Cross sections for (n,p), (n,α) and (n,2n) reactions with 14.6 MeV neutrons from the present work

Reaction	$T_{1/2}$	E_γ (KeV)	η (%)	σ (mb)
$^{90}Zr(n,p)^{90m}Y$	3.1 h	482	91	9.0±0.8
$^{91}Zr(n,p)^{91m}Y$	50.3 m	551	95	21.4±2.2
$^{92}Zr(n,p)^{92}Y$	3.53 h	934	14	20.1±1.5
$^{94}Zr(n,p)^{94}Y$	20.3 m	918	43	10.7±1.1
$^{92}Mo(n,p)^{92m}Nb$	10.16 d	934	99	68±6
$^{96}Mo(n,p)^{96}Nb$	23.4 h	569	59	18.1±1.4
$^{97}Mo(n,p)^{97g}Nb$	72 m	665	98	19.2±1.4
$^{98}Mo(n,p)^{98}Nb$	51 m	720	75	3.6±0.3
$^{90}Zr(n,\alpha)^{87m}Sr$	2.83 h	388	80	4.1±0.3
$^{94}Zr(n,\alpha)^{91}Sr$	9.67 h	1025	30	6.3±0.5
$^{96}Zr(n,\alpha)^{93}Sr$	8.3 m	888	23.7	2.4±0.3
$^{92}Mo(n,\alpha)^{89m}Zr$	4.18 m	588	87	5.6±0.5
$^{92}Mo(n,\alpha)^{89g}Zr$	78.4 h	909	99	20.1±1.6
$^{90}Zr(n,2n)^{89m}Zr$	4.18 m	588	87	86±8
$^{90}Zr(n,2n)^{89g}Zr$	78.4 h	909	99	805±58
$^{92}Mo(n,2n)^{91m}Mo$	66 s	658	54	11.8±1.2
$^{94}Mo(n,2n)^{93m}Mo$	6.9 h	685	100	2.4±0.2
$^{100}Mo(n,2n)^{99}Mo$	67 h	740	12	1420±100

η : Intensity of γ-rays per disintegration

V. NAGOYA UNIVERSITY

Department of Nuclear Engineering, Faculty of Engineering

V-1 The Decay of ^{148}Pr

H. Yamamoto, C. Ishihara, K. Kawade and T. Katoh

A paper on this subject was submitted and published in J. Phys. Soc. Japan vol. 41, no. 3, p729-734 (1976).

Decay of ^{148}Pr has been studied with Ge(Li), NaI(Tl) and plastic detectors in singles and coincidence measurements of γ-rays and β-rays. Sources were prepared by the ^{148}Nd(n,p)^{148}Pr reaction at the neutron energy of about 15 MeV. Forty-one γ-rays were observed. A decay scheme of ^{148}Pr involving 4 new levels, is proposed for the first time, and twenty γ-rays were assigned in this decay scheme. Observed Q_β value was 4.8 ± 0.2 MeV. The half-life was measured to be 2.28 ± 0.09 min.

V-2 Decay of ^{152}Pm to levels of ^{152}Sm

H. Yamamoto, K. Kawade, Y. Ikeda and T. Katoh

A paper on this subject was submitted and published in J. Phys. Soc. Japan vol. 43, no. 1, p8-16 (1977).

A spectroscopic study of the decay of ^{152}Pm to the levels of ^{152}Sm was performed by using Ge(Li), NaI(Tl) and plastic detectors. The radioactive sources were produced from the (n,p) reaction with 14.8 MeV neutrons on enriched samarium targets. The half-lives of two ^{152}Pm isomers are 4.30 ± 0.37 and 7.52 ± 0.08 min. One hundred and twenty-nine γ-rays, including 96 new ones, were observed and 108 of them are assigned to the decay schemes for ^{152}Pm including 22 new levels. An observed Q_{β} value for the 4.30 min ^{152}Pm was 3.50 $\pm$ 0.10 MeV. Most probable spin assignments of 1^{+} and 4^{-} are proposed for the 4.30 and 7.52 min ^{152}Pm, respectively. The results are discussed in terms of the unified model.

VI. TOHOKU UNIVERSITY

Department of Nuclear Engineering, Faculty of Engineering

VI-1 A study of fast neutron scattering from Be^9 at the incident energies between 3.2 MeV and 7 MeV

T. SAKASE, M. BABA, T. NISHITANI, T. YAMADA, T. MOMOTA.

In order to study the interaction of fast neutrons with Be^9, double differential neutron cross sections were measured at the incident energies, 3.2 MeV, 4.5 MeV, 6.2 MeV, and 7 MeV.

For each incident energy, energies and angular distribution of the neutrons emitted from Be^9 were measured. Neutrons were produced via the d-D reaction with the deuterium gas target and the pulsed deuteron beam from Tohoku University Dynamitron Accellerater. A conventional time-of-flight method was used for the measurement.

Cross sections were determined relative to Hydrogen cross section. From these measurement the cross sections for 1) elastic scattering, 2) inelastic scattering (Q=-2.43, -2.8, -3.03 MeV) and continuum neutron energy spectra were obtaind. Although our analysis is still preliminary the result for the elastic scatterting cross section and the spectrum of the neutrons emitted is similar to that of Marion[1) et al., and Drake et al.[2) respectively.

Analysis for inelastic scattering and continuum spectrum neutrons are now in progress.

1) J. B. MARION, J. S. LEVIN, AND L. CRANBERG. Phys. Rev., 114 1584 (1959)

2) D. M. DRAKE et al.
Nucl. Sci. Eng., 63 401 (1977)

VI-2 Gamma-Ray Production Cross Sections for Fast Neutron Interactions with Several Materials

Y.Hino, T.Yamamoto, T.Saito, N.Kishimoto,
S.Fukuda, S.Itagaki and K.Sugiyama

The differential cross sections for gamma-ray production due to fast neutron interactions have been measured at incident neutron energies of 5.8 to 7.2 MeV for aluminum and 14.7 MeV for oxygen, sodium, aluminum, chlorine, iron, copper and lead. The former measurements were performed with pulsed neutrons from the d-D reactions using the 4.5 MV Dynamitron accelerator and on the latter measurements, mono-energetic 14.7 MeV neutrons were obtained from the d-T reactions using the Cockcroft-Walton accelerator. The samples of aluminum, iron, copper and lead were made of pure metal and that of oxygen was the distilled water in a thin-walled aluminum can and of sodium and chlorine were prepared with NaCl powder compressing into the can. These samples were right cyrindrical shape of 3 cm dia. by 4 cm long. The gamma-ray spectra were measured with a heavily shielded Ge(Li) detector. Detailes of these experimental arrangements have been presented.[1] The tentative results are presented in Tables I and II.

References

1) INDC(JAP)-30"L", NEANDC(J)-44"L" (1976) and to be published in J. Nucl. Sci. Technology.

Table I.

Gamma-ray production cross sections due to fast neutron interactions with aluminum at an angle of 55°.

E_γ (keV)	Reaction types	$d\sigma/d\omega$ (mb/sr) for neutron energies (MeV) of 5.8±0.3	6.2±0.3	6.8±0.3	7.2±0.3
792	(n,n')	1.6±0.2	2.0±0.5	1.3±0.3	1.5±0.4
843	(n,n')	3.8±0.8	5.9±1.5	3.0±0.7	4.5±1.1
984	(n,p)	0.6±0.2	3.1±0.7	1.8±0.4	1.6±0.4
1013	(n,n')	10.5±2.6	14.6±3.6	11.9±2.9	13.3±3.3
1692	(n,p)		1.3±0.3	1.2±0.3	2.2±0.5
1719	(n,n')	6.4±1.6	7.7±1.9	5.4±1.3	3.6±0.9
2210	(n,n')	15.2±3.8	19.3±4.8	12.5±3.1	14.4±3.6
2300	(n,n')		1.8±0.5	1.7±0.4	2.4±0.6
2740	(n,n')	1.8±0.4			1.3±0.3
2980	(n,n')	10.9±2.7	19.3±4.8	16.5±4.1	11.2±2.8
3001	(n,n')				
3220	(n,n')		2.7±0.7	2.2±0.5	2.7±0.7
3410	(n,n')		1.6±0.4	0.9±0.3	1.3±0.3
3970	(n,n')		2.0±0.5	0.8±0.2	1.2±0.3

Table II.

Gamma-ray production cross sections for 14.7 MeV neutrons with several materials at an angle of 125°.

Element	E_γ (keV)	Reaction types	Cross sections $d\sigma/d\omega$ (mb/sr)
Oxygen	3680	$(n,\alpha)^{13}C$	5.6 ± 1.4
	3850	$(n,\alpha)^{13}C$	3.8 ± 0.9
	4430	$(n,n\alpha)^{12}C$	3.3 ± 0.8
	6130	$(n,n')^{16}O$	12.2 ± 1.2
Sodium	440	$(n,n')^{23}Na$	38.9 ± 7.8
	1270	$(n,d)^{22}Ne$	9.9 ± 2.5
	1630	$(n,n')^{23}Na$	16.1 ± 4.0
Aluminum	843	$(n,n')^{27}Al$	8.3 ± 2.1
	1013	$(n,n')^{27}Al$	8.2 ± 2.0
	1720	$(n,n')^{27}Al$	2.0 ± 0.5
	1806	$(n,d)^{26}Mg$	17.1 ± 4.3
	2210	$(n,n')^{27}Al$	15.2 ± 3.8
	3001	$(n,n')^{27}Al$	8.2 ± 2.0
Chlorine	1220	$(n,n')^{35}Cl$	3.7 ± 0.9
	1760	$(n,n')^{35}Cl$	7.7 ± 1.9
	2150	$(n,d)^{34}S$	25.4 ± 6.4
Iron	412	$(n,2n)^{55}Fe$	6.5 ± 1.6
	843	$(n,n')^{56}Fe$	72.2 ± 14.4
	928	$(n,2n)^{55}Fe$	11.3 ± 2.8
	1232	$(n,n')^{56}Fe$	31.9 ± 6.4
	1310	$(n,n')^{56}Fe$	5.3 ± 1.3
	1402	$(n,2n)^{55}Fe$	5.6 ± 1.4
	1665	$(n,n')^{56}Fe$	2.7 ± 0.7
	1802	$(n,n')^{56}Fe$	7.8 ± 1.9

Table II. (continued)

Element	E_γ (keV)	Reaction types	Cross sections $d\sigma/d\omega$ (mb/sr)
Copper	370	$(n,n')^{63}Cu$	3.5 ± 0.9
	385		7.7 ± 1.9
	960	$(n,n')^{63}Cu$	24.3 ± 6.1
	1097		2.1 ± 0.5
	1114	$(n,n')^{65}Cu$	11.1 ± 2.8
	1128	$(n,n')^{63}Cu$	3.0 ± 0.7
	1161	$(n,d)^{62}Ni$	7.1 ± 1.8
	1170	$(n,d)^{62}Ni$	20.8 ± 5.2
	1327	$(n,n')^{63}Cu$	11.5 ± 2.9
	1483	$(n,n')^{65}Cu$	5.3 ± 1.3
	1547	$(n,n')^{63}Cu$	2.7 ± 0.7
	1866	$(n,n')^{63}Cu$	3.0 ± 0.7
Lead	568	$(n,n')^{207}Pb$	104.7 ± 18.8
	800	$(n,n')^{206}Pb$	73.2 ± 14.6
	877	$(n,n')^{206}Pb$	23.4 ± 5.8
	893	$(n,n')^{207}Pb$	17.5 ± 4.4
	984	$(n,n')^{207}Pb$	23.4 ± 5.8
	1058	$(n,n')^{207}Pb$	58.5 ± 11.7
	1090	$(n,n')^{208}Pb$	20.7 ± 5.2
	1770	$(n,n')^{207}Pb$	9.3 ± 3.2
	2614	$(n,n')^{208}Pb$	23.1 ± 5.8

VI−3 Compilation of Fission Product Nuclear Data

T. Yamamoto and K. Sugiyama

Compilation of fission product nuclear data such as average decay energies of beta-ray, gamma-ray and beta+gamma, decay constants and fission yields were performed for summation calculations of decay heat. The cumulative yield of 10^{-3} % was chosen as the criteria of selecting the fission product nuclides. The total number of the nuclides amounts to 678 covering the region of mass number from 74 to 166, which contains the 91 stable and the 587 unstable nuclides. The major sources of these data were the Nuclear Data Sheets[1)] the Table of Isotopes[2)], and the table of the fission yields by Meek and Rider[3)]. New methods were applied to predict unmeasured nuclear data; one was a systematics of the ratio of the average maximum beta-ray energy to Q_β, and the other was predictions of unmeasured fission yields based on the statistical theory of nuclear fission[4)]. On the details of these methods, preliminary report was presented in elsewhere[5)] and the final paper will be published in near future.

The compiled nuclear data were used for the summation calculations of the decay heat; the results together with its uncertainty will be published in near future.

References

1) D.H. Horen et al., "Nuclear Data Sheets," ed. Nuclear Data Group, ORNL.

2) C.M. Lederer et al., "Table of Isotopes," 6th ed. (1967).

3) M.E. Meek and B.F. Rider, NEDO-12154-1 (1974).

4) T. Yamamoto and K. Sugiyama, "Nuclear Cross Sections and Technology," Washington, D.C., 1976, vol. 1, 342 (1975); J. Nucl. Sci. Technol., 11(11), 461 (1974).

5) T. Yamamoto and K. Sugiyama, Tohoku Univ., NETU-20 (1977).

VII. TOKYO INSTITUTE OF TECHNOLOGY

Research Laboratory for Nuclear Reactors

VII-1 Measurement of Neutron Capture Cross Sections from 3 to 80 KeV

N. Yamamuro, K. Saito, T. Wada, Y. Fujita* and K. Kobayashi*

The neutron capture cross sections of ^{93}Nb, ^{127}I, ^{133}Cs, ^{165}Ho, ^{181}Ta and ^{238}U from 3 to 80 KeV have been measured by time-of-flight method at the Kyoto University Research Reactor Institute 46 MeV Linear Electron Accelerator.

Capture gamma-rays emitted from samples and gamma-rays from the reaction ^{10}B(n,$\alpha\gamma$) were measured by C_6D_6 and C_6F_6 scintillation detectors. The relative capture yield obtained from these measurements was normalized to the absolute yield at 24 KeV.[1)]

The preliminary results of ^{93}Nb and ^{165}Ho agreed very well with the data of Macklin[2),3)],and the result of ^{133}Cs is about 20-30% lower than the ENDF/B-IV as shown in Fig.1. The data of ^{127}I, ^{181}Ta and ^{238}U are now being reduced.

References :

1) N. Yamamuro, et al. : Proc. of Conf. on Nuclear Cross Sections and Technology, NBS SP 425, P.802 (1975)

2) R. L. Macklin : Nucl. Sci. Eng., 59, 12 (1976)

3) R. L. Macklin : Nucl. Sci. Eng., 59, 231 (1976)

---

*Kyoto University Research Reactor Institute

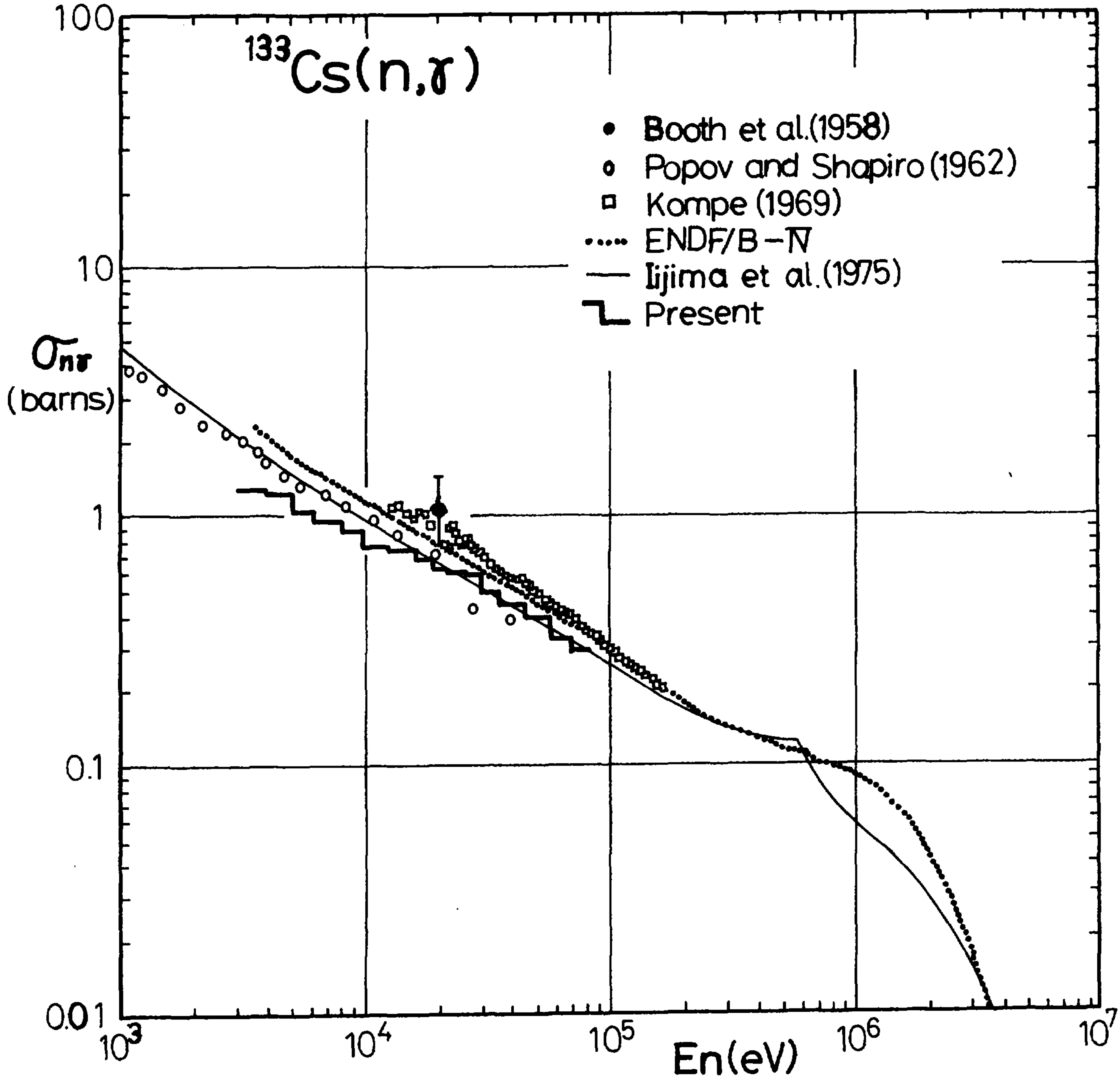

Fig.1 Neutron Capture Cross Section of ^{133}Cs

VII-2 Evaluations of Gamma-Ray Production Cross Sections for Energetic Neutrons

Y. Sano, M. Kawai*, T. Yamakoshi**, Y. Harima
H. Kitazawa, S. Iijima*, and N. Yamamuro

Gamma-ray production cross sections for energetic neutrons are needed for estimation of gamma-ray heating in the blanket of a nuclear reactor and for shield calculations. We have obtained the gamma-ray production cross sections of ^{27}Al, ^{40}Ca, ^{56}Fe, ^{93}Nb, ^{181}Ta and ^{nat}Pb, using the spin-dependent evaporation model. The calculations were made using the GROGI[1)] code, which was improved to include the Brink-Axel type resonance effect in the gamma-ray radiation width and to give the Gilbert-Cameron's formula for the nuclear level density.

The results show :

(1) Global gamma-ray spectra are well described by the evaporation model, except for discrete line spectra.

(2) Good agreement is obtained by considering the giant dipole resonance effect in the gamma-ray radiation width.

(3) The inclusion of yrast states improves the agreement between theory and experiment in lower energy gamma-ray spectra.

(4) It is useful to normalize the gamma-ray radiation width by the sum rule for radiative transition.

---

* NAIG Nuclear Research Laboratory

** Ship Research Institute

(5) Agreement for higher energy gamma-ray from heavy Nuclei is not so good.

The Figure shows the gamma-ray spectrum for ^{93}Nb irradiated with 7.01-8.02 MeV neutrons.

Reference :

1) J. Gilat : BNL-50246 (T580) (1970)

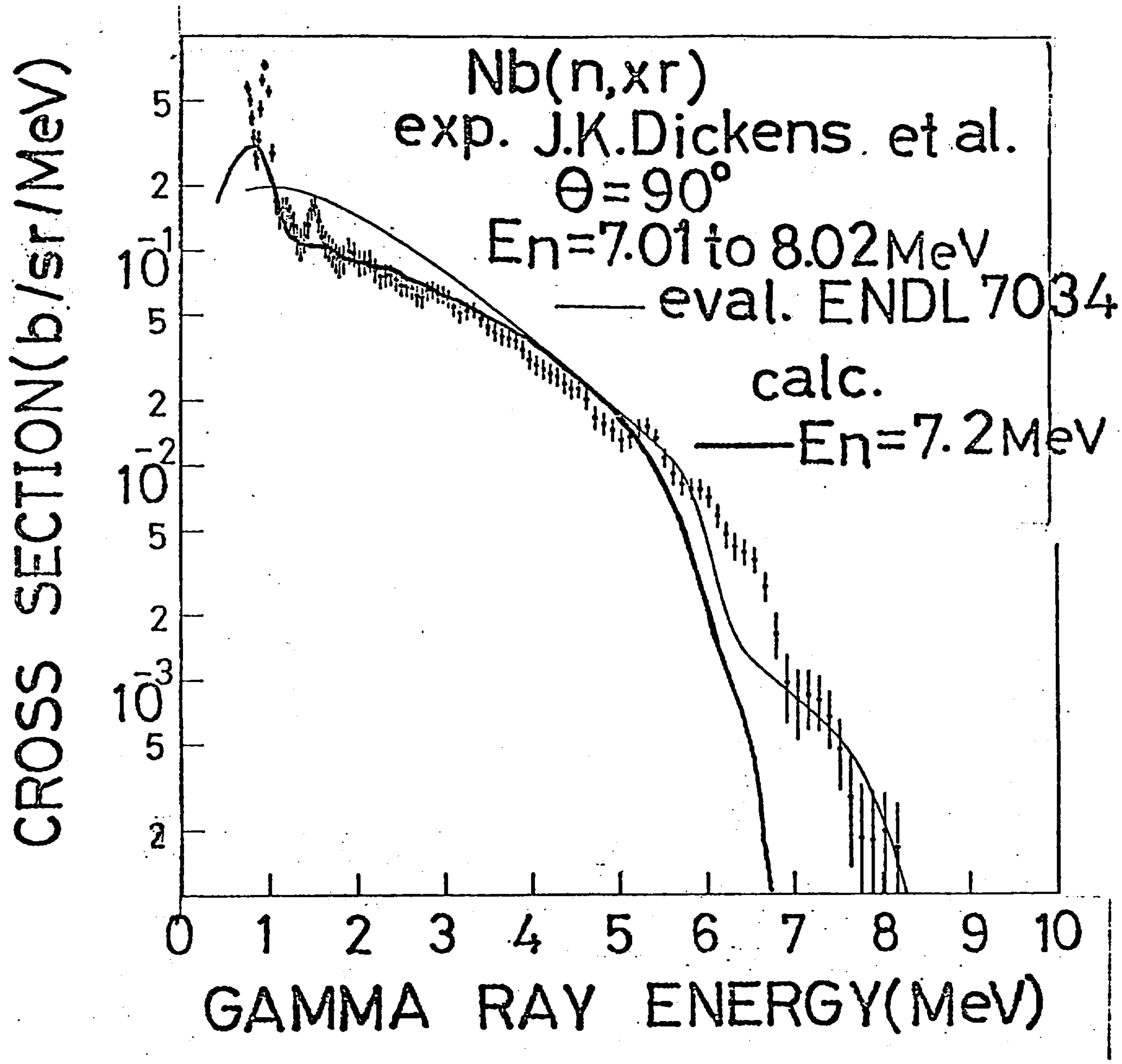

VII-3

Evaluations of the (n,p) and (n,px) Reaction Cross Sections at Threshold Energies to 20 MeV

Y. Isogai, H. Kitazawa and N. Yamamuro

We have theoretically estimated the (n,p) and (n,px) reaction cross sections of ^{48}Ti, ^{51}V, ^{52}Cr, ^{56}Fe, ^{58}Ni, ^{93}Nb, ^{98}Mo and ^{181}Ta which were used to determine the swelling of structural materials for the first wall of a fusion reactor.
The spin-dependent evaporation model[1) and the geometry-dependent hybrid model[2) for the pre-equilibrium process are used in these calculations. The evaporation model takes the competition of (n,n'),(n,p), (n,α) and (n,γ) reaction channels and the cascade process into consideration. The calculated cross sections are compared with the observed data and ENDF-III or IV. Figures show the excitation curves for these reactions. The theoretical curves are normalized by adjusting the contribution of the statistical process so that the average cross sections at 14-MeV neutron energy give the calculated values.

References :

1) J. Gilat : BNL-50246 (T-580) (1970)

2) M. Blann : Nuclear Phys. A213 (1973) 570-588

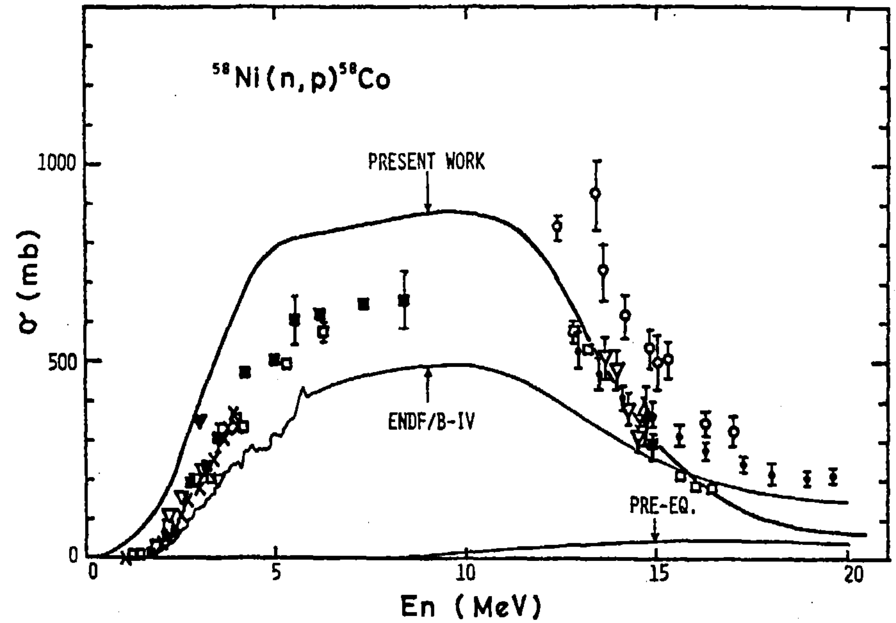
^{58}Ni(n,p)^{58}Co
PRESENT WORK
ENDF/B-IV
PRE-EQ.
σ (mb)
En (MeV)
0
500
1000
5
10
15
20

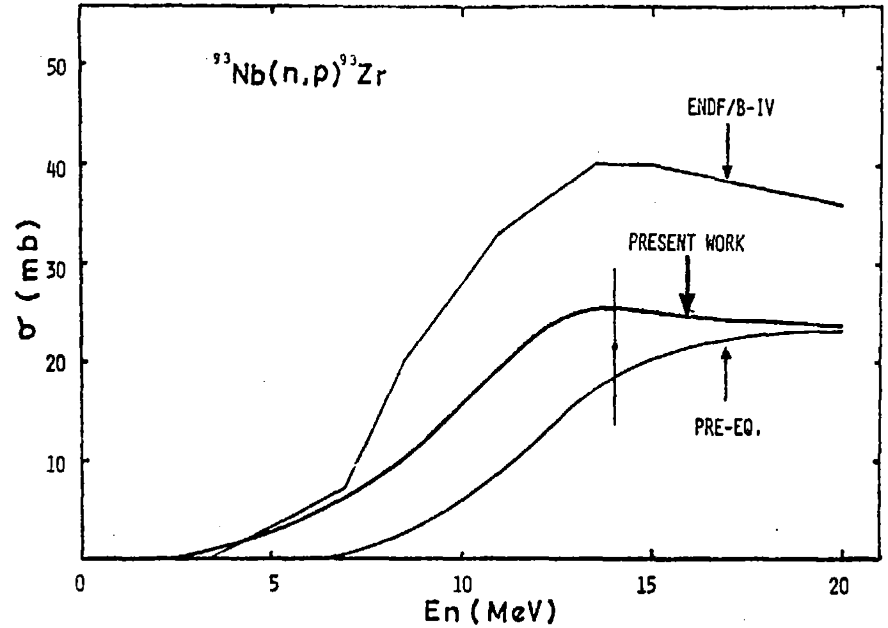
^{93}Nb(n,p)^{93}Zr
ENDF/B-IV
PRESENT WORK
PRE-EQ.
σ (mb)
En (MeV)
10
20
30
40
50
0
5
10
15
20

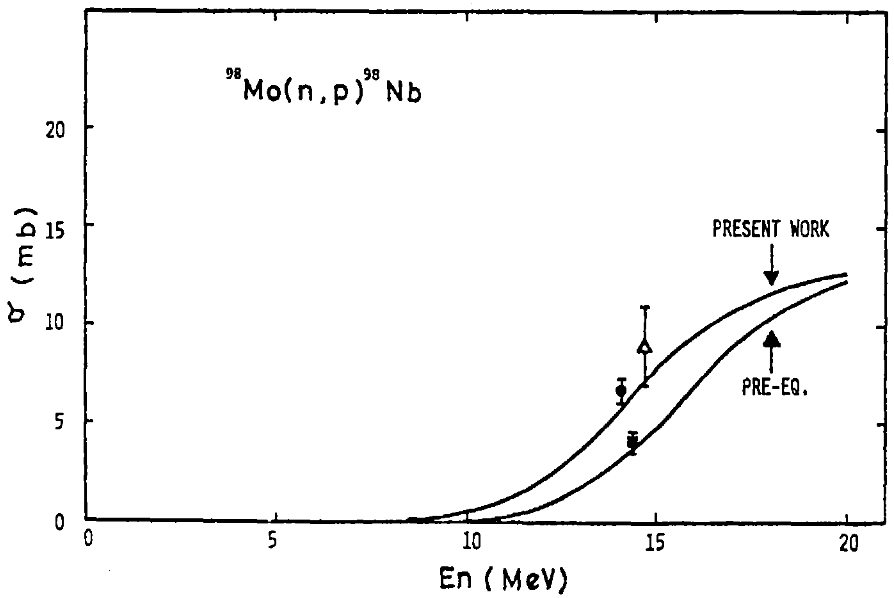
^{98}Mo(n,p)^{98}Nb
PRESENT WORK
PRE-EQ.
σ (mb)
En (MeV)
0
5
10
15
20
0
5
10
15
20

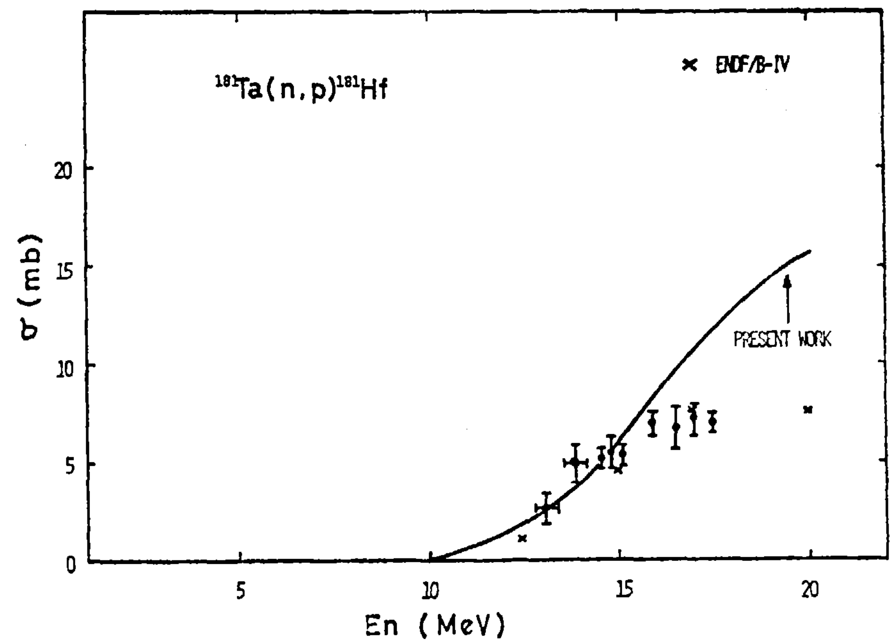
^{181}Ta(n,p)^{181}Hf
× ENDF/B-IV
PRESENT WORK
σ (mb)
En (MeV)
0
5
10
15
20
5
10
15
20

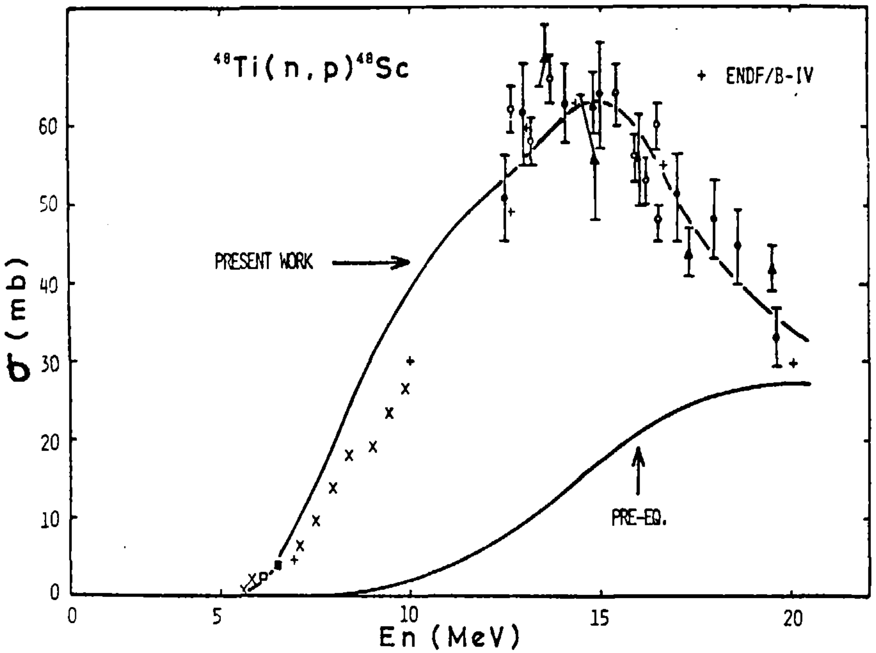

$^{48}Ti(n,p)^{48}Sc$
+ ENDF/B-IV
PRESENT WORK
PRE-EQ.
σ (mb)
En (MeV)

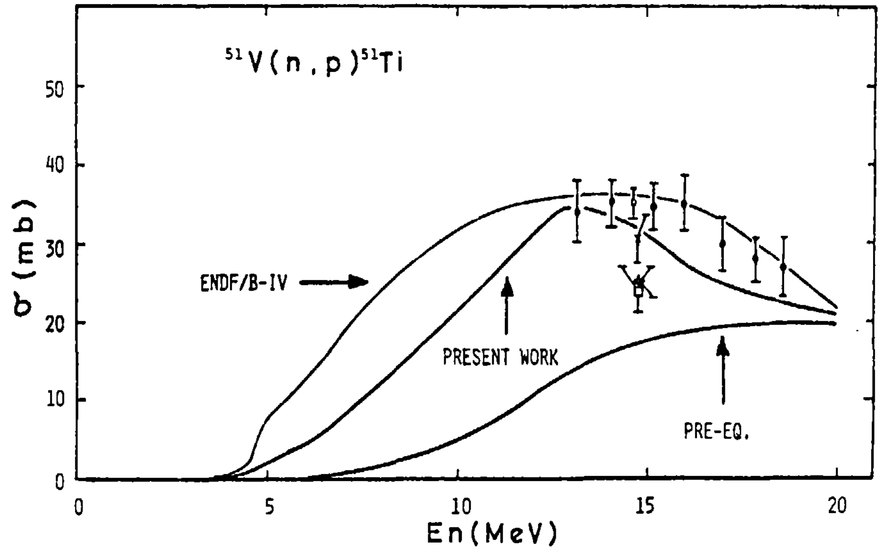

$^{51}V(n,p)^{51}Ti$
ENDF/B-IV
PRESENT WORK
PRE-EQ.
σ (mb)
En(MeV)

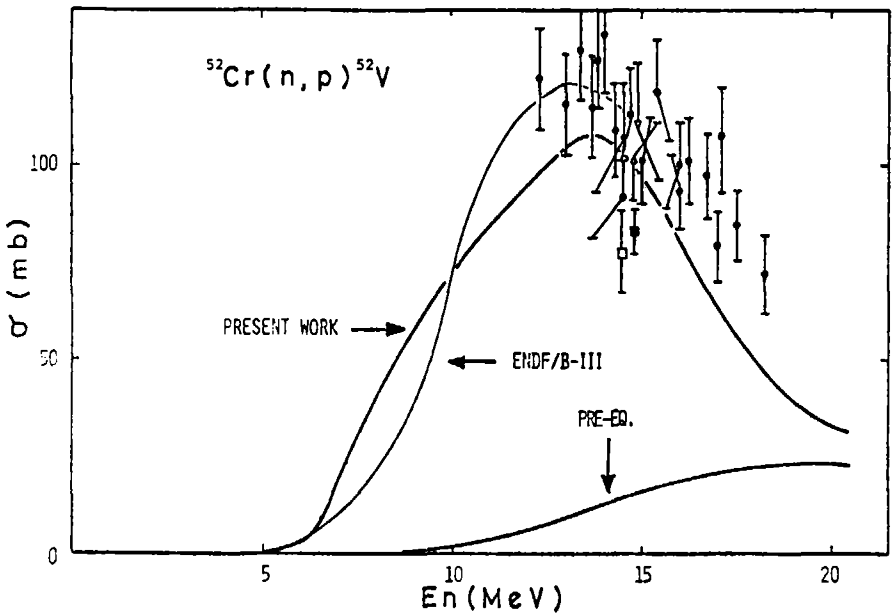

$^{52}Cr(n,p)^{52}V$
PRESENT WORK
ENDF/B-III
PRE-EQ.
σ (mb)
En(MeV)

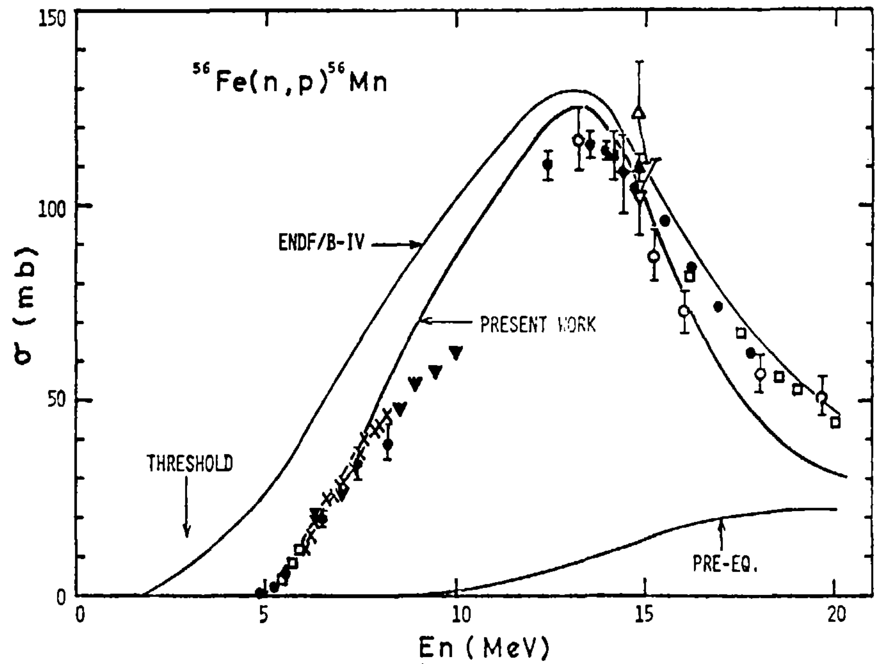

$^{56}Fe(n,p)^{56}Mn$
ENDF/B-IV
PRESENT WORK
THRESHOLD
PRE-EQ.
σ (mb)
En (MeV)